The Journal of Immunology

Antigen Receptor Specificity and Cell Location Influence the Diversification and Selection of the B-1a Cell Pool with Age

Naomi Tsuji, Thomas L. Rothstein and Nichol E. Holodick

J Immunol 2020; 205:741-759; Prepublished online 19 June 2020;
doi: 10.4049/jimmunol.1901302
http://www.jimmunol.org/content/205/3/741

The Journal of Immunology is published twice each month by
The American Association of Immunologists, Inc.,
1451 Rockville Pike, Suite 650, Rockville, MD 20852

Print ISSN: 0022-1767 Online ISSN: 1550-6606.

Antigen Receptor Specificity and Cell Location Influence the Diversification and Selection of the B-1a Cell Pool with Age

Naomi Tsuji, Thomas L. Rothstein, and Nichol E. Holodick

B-1a cells provide immediate and essential protection from infection through production of natural Ig, which is germline-like due to minimal insertion of N region additions. We have previously demonstrated peritoneal B-1a cell–derived phosphorylcholine-specific and total IgM moves away from germline (as evidenced by an increase in N-additions) with age as a result of selection. In young mice, anti-phosphatidylcholine Abs, like anti-phosphorylcholine Abs, contain few N-additions, and have been shown to be essential in protection from bacterial sepsis. In this study, we demonstrate the germline-like status of phosphatidylcholine (PtC)-specific (PtC^+) peritoneal B-1a cell IgM does not change with age. In direct contrast, the splenic PtC^+ B-1a cell population does not preserve its IgM germline status in the aged mice. Furthermore, splenic PtC^+ B-1a cells displayed more diverse variable gene segments of the H chain (V_H) use in both the young and aged mice as compared with peritoneal PtC^+ B-1a cells. Whereas the peritoneal PtC^+ population increased V_H12 use with age, we observed differential use of V_H11, V_H12, and V_H2 between the peritoneal and splenic PtC^+ populations with age. These results suggest disparate selection pressures occur with age upon B-1a cells expressing different specificities in distinct locations. Overall, these results illuminate the need to further elucidate how B-1a cells are influenced over time in terms of production and selection, both of which contribute to the actual and available natural IgM repertoire with increasing age. Such studies would aid in the development of more effective vaccination and therapeutic strategies in the aged population. ***The Journal of Immunology*****, 2020, 205: 741–759.**

Natural Abs provide the first line of defense against infection. These essential Abs are nonimmune, polyreactive, low-affinity Igs of varying isotypes found in both humans and mice (1–3). In mice, 80–90% of natural IgM is produced by B-1a cells (2, 4), which are phenotypically and functionally distinct from conventional B2 cells (5). B-1a cell–derived natural Abs provide a number of essential functions within the immune system, which include protection from infection (1), regulation of B cell development (6–8), selection of the B cell repertoire (7, 9), clearance of apoptotic debris (1), protection against atherosclerosis (10, 11), and allergic suppression (12). Notably, B-1a cell natural IgM is essential for protection against *Streptococcus pneumoniae* (13) and sepsis (14).

The incidence and mortality rate for both pneumococcal infection and sepsis increase dramatically in people over the age of 65 (aged adults) (15). Although no prophylactic treatment exists for sepsis, there is a vaccine recommended for protection from pneumococcal infection in those age 65 and over, PPSV23 (16). Despite the availability of this vaccine for aged adults since 1983, the percent of total deaths due to lower respiratory diseases has not decreased in aged adults (15). Although those over the age of 65 produce similar postvaccination Ab titers to young adults (under the age of 45), the Abs produced are less effective at clearing bacteria (17–19). Therefore, pneumococcal infections and sepsis still pose a great challenge in prevention and treatment in those over the age of 65. Natural IgM plays a role in B cell repertoire selection (7, 9) as well as T cell–independent and –dependent IgG responses (6, 9, 20–22). Importantly, studies show reduced levels of IgG after immunization (6, 9) or infection (20–22) in the absence of natural IgM. In addition, B-1 cells produce natural Abs that are highly effective at providing protection against both pneumococcal infections and sepsis; however, how these B cells and/or the natural Abs they produce are affected by age is still being explored. Because natural IgM plays a number of vital roles within the immune system, and older individuals respond poorly to pneumococcal vaccination, it is critical to understand how B-1a cell–derived natural IgM changes with age.

The ability of B-1a cell–derived natural IgM to effectively clear *S. pneumoniae* and sepsis infections is attributed to its unique germline structure and specificities, which are capable of binding bacterial and mammalian cell membrane components. Such specificities include phosphorylcholine (PC) (23) and phosphatidylcholine (PtC) (24). PC is a principal Ag found on the cell wall of *S. pneumoniae*. PtC is an Ag exposed on the surface of senescent RBCs and bacterial cell membranes (24). Anti-PtC Abs have been shown to be essential in protection from bacterial sepsis (14). The structure of natural IgM is termed germline-like because of minimal insertion of nontemplate-encoded N nucleotides (N region additions) along with little somatic hypermutation (25). N-additions are added to the V-D and D-J junctions by the enzyme TdT (25, 26) and play a key role in AgR diversification. B-1a cells originate mainly during fetal life and persist throughout adult life primarily by self-renewal. During fetal development, TdT is not expressed; therefore, mature fetal-derived

Center for Immunobiology, Western Michigan University Homer Stryker M.D. School of Medicine, Kalamazoo, MI 49007; and Department of Investigative Medicine, Western Michigan University Homer Stryker M.D. School of Medicine, Kalamazoo, MI 49007

ORCID: 0000-0002-2671-6918 (N.E.H.).

Received for publication October 28, 2019. Accepted for publication May 20, 2020.

This work was supported by Division of Intramural Research, National Institute of Allergy and Infectious Diseases, National Institutes of Health, Public Health Service Grant AI142004.

Address correspondence and reprint requests to Dr. Nichol E. Holodick, Western Michigan University Homer Stryker M.D. School of Medicine, 1000 Oakland Drive, Kalamazoo, MI 49008. E-mail address: nichol.holodick@med.wmich.edu

The online version of this article contains supplemental material.

Abbreviations used in this article: D_H, diversity gene segment of the H chain; DMPC, 1,2-dimyristoyl-*sn*-glycero-3-phosphocholine; DOPC, 1,2-dioleoyl-*sn*-glycero-3-phosphocholine; J_H, joining gene segment of the H chain; PC, phosphorylcholine; PtC, phosphatidylcholine; RF, reading frame; V_H, variable gene segment of the H chain.

B-1a cells developed during fetal life lack N-additions. The prototypical B-1a anti-PC Ab T15 has no N-addition and is highly protective against *S. pneumoniae* infection (27, 28). Mice expressing TdT constitutively (TdT-transgenic mice) fail to produce germline Ab (Ab lacking N-additions). Notably, TdT-transgenic mice vaccinated with heat-killed *S. pneumoniae* generated an anti-PC response; however, these anti-PC Abs containing abundant N-additions were not protective against *S. pneumoniae* infection (29). Anti-PtC Abs, like anti-PC Abs, also contain very few N-additions (30) and are protective against sepsis (14). These studies highlight the importance of Ab structure in terms of germline status for providing protection against infection.

We and others have previously shown the germline-like (few N-additions) structure of peritoneal B-1a cell–derived natural IgM in young 2- to 3-mo-old mice moves away from germline (increase in N-additions) by 6 mo of age (mature adult mice) (31–33). This change away from germline in peritoneal B-1a cells is maintained into old age (18–24 mo) (33). Furthermore, we demonstrated this increase in N-additions observed in IgM from the total peritoneal B-1a cell population was also observed in PC-specific peritoneal B-1a cell IgM with age (33). We subsequently showed the protective capacity of natural serum IgM diminishes with advancing age, and the changes in germline status of natural IgM in the aged population are a consequence of selection pressures acting upon the peritoneal B-1a cell pool, which is composed of both fetal- and adult-derived B-1a cells (33).

Approximately 5–15% of the peritoneal B-1a cell population is specific for PtC, which has particular heavy and L chain pairings permissive during fetal life (30). In light of extensive literature demonstrating the major role selection plays in shaping the B-1a cell pool, we questioned how the PtC-binding B-1a cell population would be affected over time. To examine this, we performed single-cell sequencing on PtC- and PC-specific B-1a cells from young (3-mo-old), aged (18-mo-old), and middle-aged (10–16 mo old) BALB/c-ByJ mice. In the analysis performed in this study, we find the specificity and location of B-1a cells determines how the population is affected by age and selection over time. Importantly, we demonstrate an age-associated loss of a particular CDR-H3 specificity in peritoneal B-1a cells. Loss of such specificities in the aged mice has implications for susceptibility to infection and/or other diseases common to the aged mice. Our study greatly extends our understanding of how this important innate B cell subset is affected during advancing age.

Materials and Methods

Mice

Male BALB/cByJ mice were obtained from The Jackson Laboratory at 6–8 wk of age and were aged in our vivarium for the times indicated. The mice were housed at five mice per cage with a 12 h light/12 h dark cycle and ad libitum access to water and food. Mice were cared for and handled in accordance with the Guide for the Care and Use of Laboratory Animals, National Institutes of Health, and institutional guidelines. All animal studies were approved by the Institutional Animal Care and Use Committee.

Cell purification and flow cytometry

Peritoneal lavage and spleen removals were performed on all euthanized mice. Spleens were homogenized using the rough ends of glass slides or the Miltenyi gentleMACS dissociator and then passed through a 70-μm cell strainer. All samples were treated with RBC lysis buffer for 2 min (Lonza), subsequently diluted with HBSS with 2.5% FBS, and then centrifuged at 1200 rpm for 10 min. The cells were resuspended in HBSS with 2.5% FBS, stained with immunofluorescent Abs, and then analyzed on an LSRII Flow Cytometer or Influx cell sorter (BD Biosciences) with gating on live cells by forward side scatter and/or Aqua Live/Dead stain (Invitrogen). Images were constructed with FlowJo 10.0 software (Tree Star, San Carlos, CA). The following Abs were obtained from BD Pharmingen: CD19 (clone ID3), CD43 (clone S7), B220/CD45 (clone RA3-6B2), CD23 (clone B3B4), and CD5 (clone 53-7.3). For PtC and PC staining, the following items were used: FITC-labeled PtC liposomes (kindly provided by Dr. S. Clark and Dr. A. Kantor) diluted at 1:30,000; PE-Cy7–labeled PC-BSA; and FITC-labeled BSA used at 10 μg/ml (PC^+ BSA^- B-1a cells were used for sorting). The composition of the PtC liposomes used is DSPC/DSPG/Chol (molar ratio: 45:5:50).

Single-cell sequencing and analysis

Peritoneal washout cells and splenocytes were obtained from BALB/c-ByJ mice at the indicated age and stained with fluorescence-labeled Abs. B-1a cell populations were single-cell sorted using an Influx Cell Sorter (BD Biosciences) into a 96-well plate containing lysis buffer (RNaseOut, 5× buffer, DTT, IgePAL, carrier RNA; Invitrogen). Postsort reanalysis of B-1a cell populations showed them to be ≥98% pure. To obtain cDNA, a 20-μl reverse transcription reaction was run per well using the SuperScript III enzyme and random hexamers (Invitrogen).

H chain analysis. Qiagen's HotStart Taq Plus Master Mix Kit was used to perform the first round of PCR (25-μl reaction) using 2.5 μl of cDNA diluted 1:2 and the following primers: MsV_HE and MsCμE, each at 0.6 μM, as previously described (26). Each 25-μl reaction was run as follows: 95˚C for 5 min; 35 cycles at 94˚C for 30 s, 50˚C for 30 s, and 72˚C for 30 s; and then a final extension at 72˚C for 10 min. The product from this first reaction was then diluted at 1:100 in dH_2O and 2 μl was used in the second seminested 25-μl reaction using the following primers: MsV_HE and MsCμN, each at 0.6 μM, as previously described (26). The second reaction was run as follows: 95˚C for 5 min; 40 cycles at 94˚C for 30 s, 53˚C for 30 s, and 72˚C for 30 s; and then a final extension at 72˚C for 10 min. The products were run on the Qiagen Qiaxcel. PCR products were sequenced (Genewiz) using the MsV_HE primer. Sequences were analyzed using an online sequence analysis tool, IMGT/HighV-Quest (34).

κ L chain analysis. Qiagen's HotStart Taq Plus Master Mix Kit was used to perform the first round of PCR (25-μl reaction) using 2.5 μl of cDNA diluted 1:2 and primers the following primers: LV_k3, LV_k4, LV_k5, LV_k6, LV_k789, LV_k14, LV_k19, LV_k20, and mC_k at 200 nM, as previously described (35). Each 25-μl reaction was run as follows: 94˚C for 15 min; 50 cycles at 94˚C for 30 s, 50˚C for 30 s, and 72˚C for 55 s; and then a final extension at 72˚C for 10 min. The product from this first reaction was then diluted at 1:100 in dH_2O and 2 μl was used in the second seminested 25-μl reaction using the following primers: $V_κ$, J_k01, J_k02, J_k03, and J_k04 at 200 nM, as previously described (35). The second reaction was run as follows: 94˚C for 15 min; 50 cycles at 94˚C for 30 s, 69˚C for 30 s, and 72˚C for 45 s; and then a final extension at 72˚C for 10 min. The products were run on the Qiagen Qiaxcel. PCR products were sequenced (Genewiz) using the $V_κ$ primer. Sequences were analyzed using an online sequence analysis tool, IMGT/HighV-Quest (34).

Lambda L chain analysis. Qiagen's HotStart Taq Plus Master Mix Kit was used to perform the first round of PCR (25-μl reaction) using 2.5 μl of cDNA diluted 1:2 and the following primers: $mV_{lambda}1/2$, $mV_{lambda}X$, and mC_{lambda}outter at 200 nM, as previously described (35). Each 25-μl reaction was run as follows: 94˚C for 15 min; 50 cycles at 94˚C for 30 s, 58˚C for 30 s, and 72˚C for 55 s; and then a final extension at 72˚C for 10 min. The product from this first reaction was then diluted at 1:100 in dH_2O and 2 μl was used in the second seminested 25-μl reaction using the following primers: $mV_{lamda}1/2$, $mV_{lambda}X$, and mC_{lambda}inner at 200 nM, as previously described (35). The second reaction was run as follows: 94˚C for 15 min; 50 cycles at 94˚C for 30 s, 66˚C for 30 s, and 72˚C for 30 s; and then a final extension at 72˚C for 10 min. The products were run on the Qiagen Qiaxcel. PCR products were sequenced (Genewiz) using the $mV_{lamda}1/2$ primer. Sequences were analyzed using an online sequence analysis tool, IMGT/HighV-Quest (34).

ELISPOT assay

ELISPOT assay was carried out as previously described (36). In brief, sort-purified, naive B cells were distributed onto MultiScreen-IP Plates (Millipore) precoated with goat anti-mouse Ig (H + L) and then incubated in RPMI 1640 containing 10% heat-inactivated FBS, 2 mM L-glutamine, 50 μM 2-ME, 100 U/ml penicillin, and 100 μg/ml streptomycin for 4 h at 37˚C and 5% CO_2. Plates were treated with alkaline phosphatase-conjugated goat anti-mouse IgM (Southern Biotechnology Associates) and developed with 5-bromo-4-chloro-3-indolyl phosphate/p-NBT chloride substrate (KPL). IgM-secreting B cells were enumerated using the Immunospot S6 analyzer (Cellular Technology).

*1,2-Dimyristoyl-*sn*-glycero-3-phosphocholine and 1,2-dioleoyl-*sn*-glycero-3-phosphocholine ELISA analysis*

Serum was collected from individual BALB/c-ByJ naive mice at the time of euthanasia at the ages indicated. The serum was analyzed for Ab against

1,2-dimyristoyl-*sn*-glycero-3-phosphocholine (DMPC) and 1,2-dioleoyl-*sn*-glycero-3-phosphocholine (DOPC) by ELISA. ELISA strips were obtained from Avanti Polar Lipids precoated with DMPC or DOPC. The wells were blocked with 200 μl of 3% fatty acid–free BSA in PBS for 1 h at room temperature with gentle shaking. The wells were then washed three times with 1× PBS. Diluted serum was added at 50 μl per well and incubated for 1 h at room temperature with gentle shaking. The wells were then washed three times with 1× PBS. Bound Ab was measured using HRP-conjugated goat anti-mouse IgM (Bethyl Laboratories) at 1:20,000. The NC-17D8 Ab (VH11/Vκ9-expressing IgM), kindly provided by Dr. G. Silverman, was used as a standard and included on each plate.

Statistics

Comparisons were conducted as indicated using Graphpad Prism 8.0. χ^2 analysis was performed using 2×4 comparisons as indicated. The Mann–Whitney *U* test was performed on data without a normal distribution as indicated.

Results

The germline-like structure of IgM from peritoneal cavity PtC–binding B-1a cells does not change in the aged mice

It has been shown that PtC-binding B-1a cells develop mainly during fetal life and are rarely supplemented or replaced during adulthood by bone marrow–derived B cells but are maintained primarily by self-renewal (30). We first assessed the peritoneal B-1a cell pool for repertoire skewing in the aged mice toward PtC using fluorescently labeled PtC liposomes (37). Fig. 1A displays a representative gating strategy. We found the average percent of peritoneal B-1a cells binding PtC liposomes did not change in aged mice (mean of 14.7% ± 1.39 SEM in aged versus 15.3% ± 2.27 SEM in young mice) (Fig. 1B). Next, we evaluated the structure of IgM from PtC-binding (PtC^+) and PtC-nonbinding (PtC^-) peritoneal B-1a cells from young (3-mo-old) and aged (15- to 18-mo-old) BALB/c-ByJ mice by single-cell PCR. Please note, we observe no difference in the repertoire or germline-like status from middle-aged mice (10–14 mo) as compared with aged mice (18–24 mo), which we previously reported for total B-1a cells (33); therefore, for this study, we combine these age groups. As we and others have previously shown, N-additions in IgM from the total B-1a cell population and the PC-binding B-1a cell population increase in number with age (31–33). In contrast, we found no significant increase in N-addition with age in IgM derived from PtC^+ B-1a cells (Fig. 1). Fig. 1C shows 61% of sequences from young peritoneal PtC^+ B-1a cells lack N-additions at both junctions, whereas 63% of sequences from aged peritoneal PtC^+ B-1a cells completely lack N-additions. However, the PtC^- B-1a cell population gained a significant number of N-additions with age (58 versus 41% of sequences lack all N-additions, $p < 0.0270$, χ^2, 2×4) (Fig. 1C). Examining the junctions independently (Fig. 1D), the IgM from PtC^+ B-1a populations in the young and aged populations showed similar N-addition length. In contrast, IgM from PtC^- B-1a cells displayed an increase in N-addition length at the V-D junction (young mean length = 0.975 ± 0.159 SEM versus aged mean length = 1.89 ± 0.202 SEM, $p = 0.0017$) and at the sum of the two junctions (young mean length = 1.60 ± 0.232 SEM versus aged mean length = 2.88 ± 0.285 SEM, $p = 0.0015$). These results demonstrate the structure of IgM from the PtC^+ B-1a cell population remains germline-like in the aged population. Peritoneal cavity PtC^+ B-1a cells make up, on average, 15% of total peritoneal B-1a cells in the young and aged mice. Therefore, in aged mice, the majority of peritoneal B-1a cell IgM derives from PtC^- B-1a cells producing Abs that have moved away from the germline. The findings regarding PtC^- B-1a cells (the bulk of peritoneal B-1a cells) are in agreement with our previously published observations on IgM from total and PC-specific peritoneal B-1a cells (33). In direct contrast, the peritoneal PtC^+ B-1a cell population preserves its germline-like status in the aged mice.

Repertoire of peritoneal cavity B-1a cell PtC binders changes in the aged mice

Examination of the variable gene segments of the H chain (V_H), diversity gene segments of the H chain (D_H), and joining gene segments of the H chain (J_H) from PtC binders and nonbinders in young and aged mice revealed differences in V_H, D_H, and J_H usage between young and aged mice (Fig. 2). Aged peritoneal PtC^+ B-1a cells used V_H12 more frequently than young peritoneal PtC^+ B-1a cells (31% in aged versus 7% in young mice, $p < 0.0001$), whereas the young peritoneal PtC^+ B-1a cells used V_H2 more frequently than aged peritoneal PtC^+ B-1a cells (55% in young versus 31% in aged mice, $p \leq 0.0001$). Peritoneal PtC^- B-1a cells from young mice also used V_H2 more frequently than peritoneal PtC^- B-1a cells from the aged (28% in young versus 17% in aged mice, $p = 0.0299$). These results are shown in Fig. 2A.

This shift in V_H use is due to an increase in replicate sequences, meaning sequences with the exact same CDR-H3 sequence (same V_H, D_H, J_H, N-additions, and P-insertions). We refer to these sequences as replicates instead of clones because we observe diversity in L chain use within these replicates (Supplemental Fig. 1). Of the 166 total sequences from young peritoneal PtC^+ B-1a cells, 90 were replicate sequences (54%). Of the 347 total sequences from aged peritoneal PtC^+ B-1a cells, 248 were replicate sequences (71%). Interestingly, the frequency of replicate sequences in young and aged peritoneal PtC^- B-1a cell IgM (20 versus 36%, respectively) was less than that seen in PtC^+ B-1a cells (54 versus 71%, respectively). These data are summarized in Table I. Of the replicates seen in aged peritoneal PtC^+ B-1a cells, V_H2, V_H11, and V_H12 are the most abundantly used (Fig. 2B, Table I). Furthermore, there is an increase in diversity (unique CDR-H3 sequences) within the replicate sequences in aged mice, which is demonstrated in Fig. 2C with each color representing a unique CDR-H3 amino acid sequence. Interestingly, within the replicate sequences of PtC^+ B-1a cells, there is a significant increase in V_H12 (from 3 to 97 sequences) with age, which consists of eight unique CDR-H3 amino acid sequences (Table I). There are also a number of replicate sequences utilizing V_H11 within this aged population (76 sequences), which consists of 10 unique CDR-H3 amino acid sequences (Table I). These results, along with L chain analysis (Supplemental Fig. 1), suggest there is not a monoclonal expansion of PtC^+ B-1a cells using V_H11 or V_H12 in the aged mice. Thus, our results indicate the overuse of V_H12 in the aged mice is due to oligoclonal expansion. Interestingly, two groups have independently shown overuse of a specific CDR-H3 amino acid sequence (MRYGNYWYFDV) within the young B-1a cell population (38, 39), which utilizes V_H11-D_H2-J_H1. Remarkably, this specificity was shown to bind PC and OxLDL epitopes in addition to classical PtC epitopes (38). We also observe this sequence within the young and aged peritoneal PtC^+ B-1a cell population and demonstrate it is solely within the PtC^+ population; it is not present in the young or aged peritoneal PtC^- B-1a cell population (Table I, CDR-H3 in bold type). Comparing sequences we obtained from peritoneal PC^+ B-1a cells (33) versus peritoneal PtC^+ B-1a cells (Fig. 2), we found a few identical CDR-H3 sequences shared between PC- and PtC-specific peritoneal B-1a cells in the young and aged mice (Supplemental Fig. 2A). These results demonstrate of all PC and PtC sequences there are 1.5% identical CDR-H3 amino acid sequences shared between PC- and PtC-specific B-1a cells in the young, whereas 1.9% are shared between the aged populations of PC and PtC B-1a cells. The prominent MRYGNYWYFDV sequence was found in both

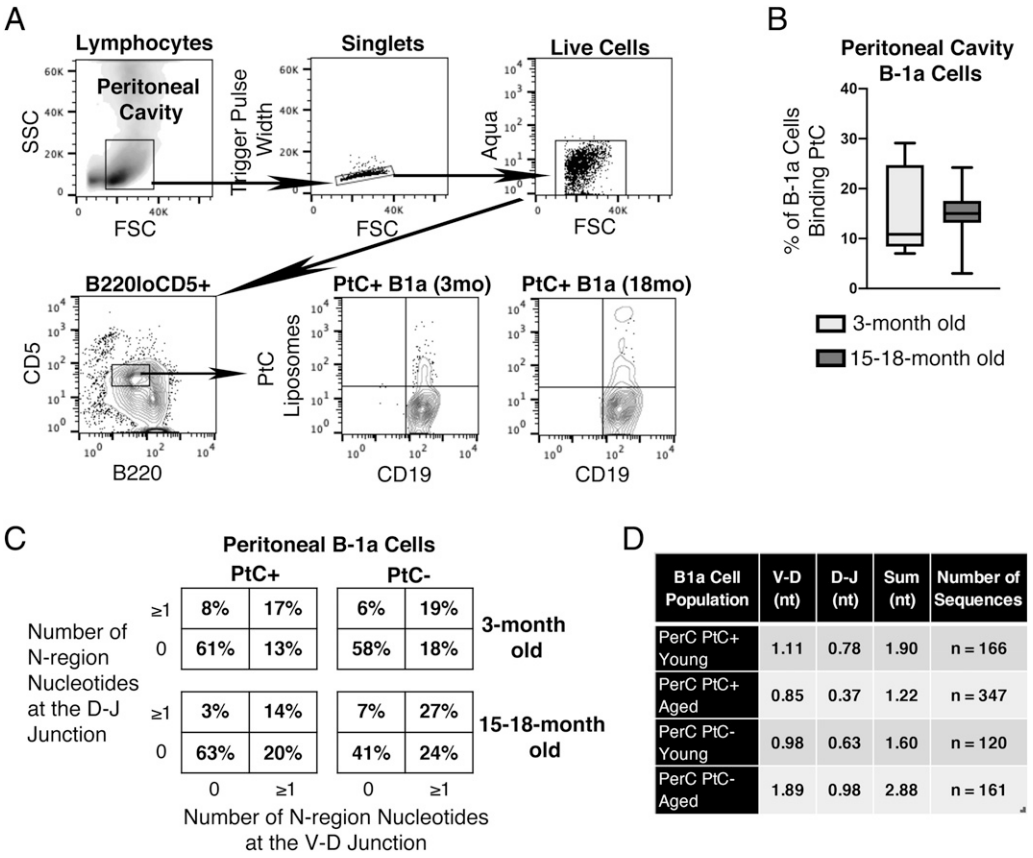

B1a Cell Population	V-D (nt)	D-J (nt)	Sum (nt)	Number of Sequences
PerC PtC+ Young	1.11	0.78	1.90	n = 166
PerC PtC+ Aged	0.85	0.37	1.22	n = 347
PerC PtC- Young	0.98	0.63	1.60	n = 120
PerC PtC- Aged	1.89	0.98	2.88	n = 161

FIGURE 1. Peritoneal PtC$^+$ and PtC$^-$ B-1a cell IgM differ in germline status in aged mice. Peritoneal washouts were obtained from 3- or 15- to 18-mo-old BALB/c-ByJ male mice and analyzed for PtC positive B-1a cells by immunofluorescent staining. (**A**) Representative gating strategy for analysis and sorting of peritoneal PtC$^+$ and PtC$^-$ B-1a cells. (**B**) Average percent of peritoneal B-1a cells binding PtC liposomes (±SEM). (**C** and **D**) PtC$^+$ and PtC$^-$ B-1a cells were single-cell sorted from 3- and 15- to 18-mo-old (as indicated) male BALB/c-ByJ mice. The V_H region was amplified and sequenced as detailed in *Materials and Methods*. (C) The percent of sequences with zero N-additions at both junctions, one or more N-additions at both junctions, zero N-additions at V-D and one or more at D-J junctions, or zero N-additions at D-J and one or more at V-D junctions is shown. (D) Average number of N-additions at the V-D, D-J, or sum of the two junctions. Results are based on three independent experiments with sequences combined from each independent experiment ($n = 7$ for 3-mo-old mice; $n = 11$ for 15- to 18-mo-old mice). Statistics used: (B and D) Mann–Whitney U test and (C) 2×4 χ^2 test.

PC- and PtC-specific B-1a cell populations in the young and aged mice (Supplemental Fig. 2A). These findings are in line with the recent work by Prohaska et al. (38), showing the classic PtC CDR-H3 MRYGNYWYFDV could bind both PtC and PC epitopes. Importantly, the frequency of this amino acid sequence among all sequences decreases in the aged PtC$^+$ B-1a cells (17% in the young to 10% in the aged). This decrease is more pronounced when examining the frequency among the replicate sequences in the young versus aged PtC$^+$ B-1a cells (32 versus 13%, respectively). The age-associated skewing of this specificity could have important implications for how protective Abs are maintained with age.

Because of the large number of replicate sequences seen in our results, we determined if the germline status of these subsets was skewed by the replicate sequences. Therefore, we performed N-addition analysis including only one representative replicate sequence of each unique replicate set. This analysis demonstrated the same lack of change in germline status in the aged PtC$^+$ peritoneal B-1a cell population and a change away from germline in the PtC$^-$ peritoneal B-1a cell population (Fig. 2D). This increase in replicate sequences, especially in the PtC$^+$ population, fits with the B-1a cell population being a self-renewing pool of cells. For this reason, we continue our analysis with all replicate sequences included.

Examination of the D_H and J_H genes shows significant differences in use in the aged versus young peritoneal PtC$^+$ populations. The aged peritoneal PtC$^+$ B-1a cells display an increase in D_H4 use (10% in aged versus 1% in young mice, $p < 0.0001$) and a decrease in D_H2 use (32% in aged versus 46% in young mice, $p = 0.0044$) as compared with young peritoneal PtC$^+$ B-1a cells (Fig. 2E). The aged peritoneal PtC$^+$ B-1a cells display an increase in J_H1 use (61% in aged versus 47% in young mice, $p = 0.0032$) and a decrease in J_H4 use (25% in aged versus 40% in young mice, $p < 0.0001$) as compared with young peritoneal PtC$^+$ B-1a cells (Fig. 2F). There were no significant differences observed in D_H or J_H use between young and aged mice in the peritoneal PtC$^-$ B-1a cells (Fig. 2E, 2F). Recall, J_H1 and D_H4 (DQ52) usage are associated with early/fetal life, and such J_H/D_H–biased usage becomes normalized in the adult via selection (31, 40, 41). The increase in D_H4 and J_H1 we observe in this study reflects the increase in V_H12 replicates (Table I) observed in the aged peritoneal PtC$^+$ B-1a cell population. Therefore, in the aged peritoneal PtC$^+$ B-1a cell population there is an increase in fetal rearrangements using V_H12, D_H4, and J_H1 as a result of selection, which has been previously shown for V_H12 in older mice (42).

Overall, these results demonstrate differential selection of PtC$^+$ and PtC$^-$ B-1a cells in the peritoneal cavity with increasing age. Peritoneal PtC$^-$ B-1a cells displayed little change in VDJ usage despite significant changes in germline-like status (increase in N-additions) with age. In contrast, peritoneal PtC$^+$ B-1a cells displayed significant changes in VDJ usage and no changes in germline-like status with age. Together these finding demonstrate

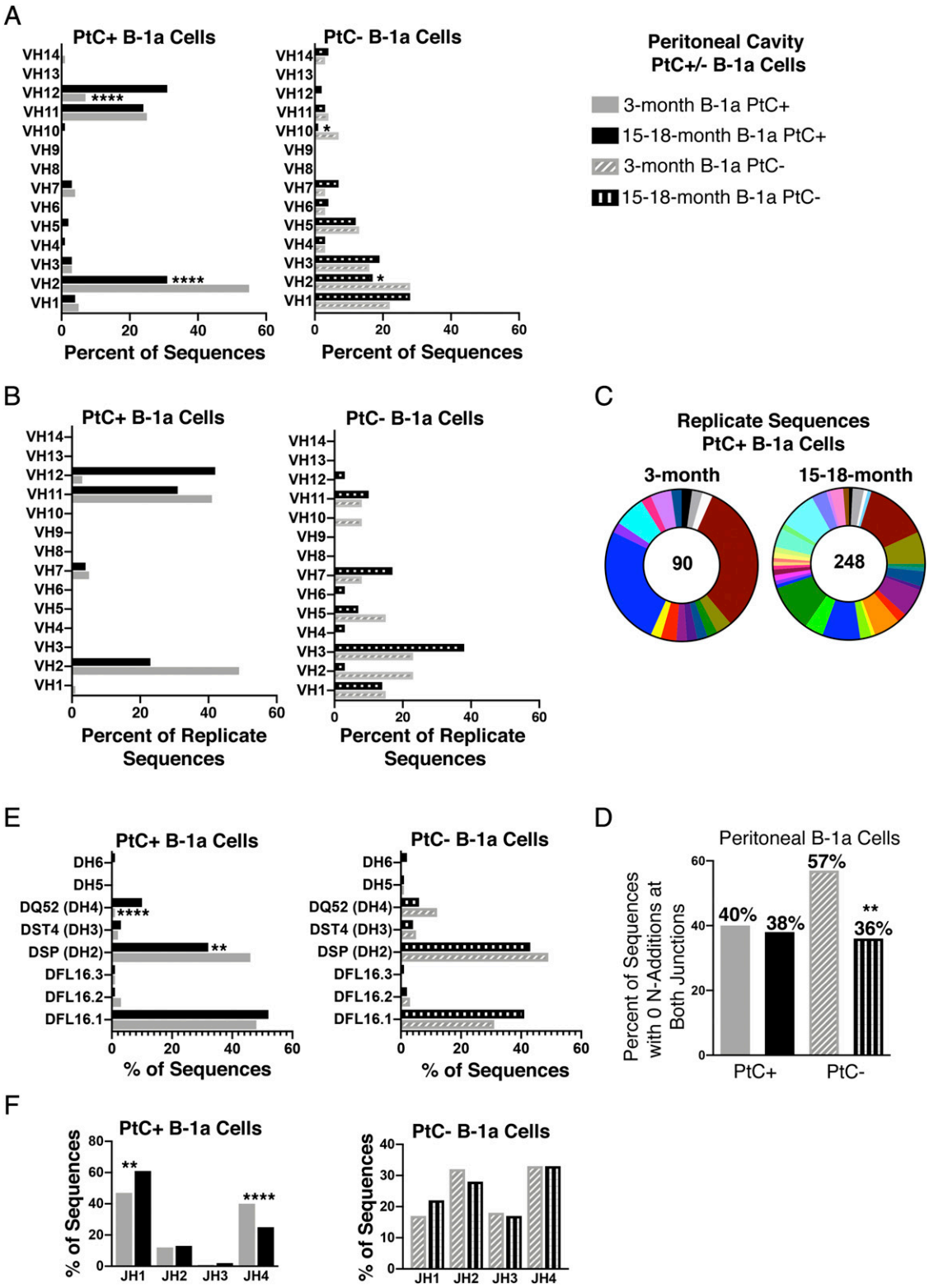

FIGURE 2. Repertoire analysis of natural IgM from peritoneal PtC^+ and PtC^- B-1a cells in aged and young adult mice. PtC^+ and PtC^- B-1a cells were single-cell sorted from 3- and 15- to 18-mo-old (as indicated) male BALB/c-ByJ mice. The V_H region was amplified and sequenced as detailed in *Materials and Methods*. (**A**) The percent of V_H gene segment usage. (**B**) The percent of V_H gene segment usage within the replicate sequences is displayed. (**C**) Distribution of replicate CDR-H3 sequences in the young and aged mice (number in the middle represents the number of replicates within the population). Each color represents a unique CDR-H3 amino acid sequence. (**D**) The percent of sequences containing zero N-additions at both junctions is shown without replicate sequences included in the analysis. (**E**) The percent of D_H gene segment usage. (**F**) The percent of J_H gene segment usage. Results are based on three independent experiments with sequences combined from each independent experiment ($n = 7$ for 3-mo-old mice; $n = 11$ for 15- to 18-mo-old mice). Statistics used: 2×2 χ^2 test. $^{**}p \leq 0.01$, $^{****}p \leq 0.0001$ (exact p values are defined in the text).

Table I. Replicate sequences within peritoneal PtC$^+$ and PtC$^-$ B-1a cells

Sample	V-D-J	CDR-H3	Total No. of Sequences with CDR-H3	Total No. of Unique Sequences[a]	Total No. of Replicate Sequences[b]
Peritoneal PtC$^+$ young				166	90 (54%)
	V_H1-D_H2-J_H1	ARRYDGYYSYWYFDV	2		
	V_H11-D_H2-J_H1	TSYGNYWYFDV	2		
	V_H11-D_H2-J_H1	MRYGNSWYFDV	2		
	V_H11-D_H2-J_H1	**MRYGNYWYFDV**	**29**		
	V_H12-D_H1-J_H1	AGDYYGYWYFDV	3		
	V_H2-D_H1-2-J_H4	ARNSLLRLLYYYAMDY	2		
	V_H2-D_H1-1-J_H1	AKIYYYGSSYFDV	2		
	V_H2-D_H1-1-J_H4	AIYYYGSSLYYAMDY	2		
	V_H2-D_H1-1-J_H4	ASHLLLRYYAMDY	2		
	V_H2-D_H1-1-J_H4	ARDYYGSYYAMDY	3		
	V_H2-D_H1-1-J_H4	ARGPALITTVYAMDY	2		
	V_H2-D_H1-1-J_H4	ARDYYGSSYYAMDY	23		
	V_H2-D_H1-1-J_H4	ARDLYYYGSSYAMDY	2		
	V_H2-D_H2-J_H4	ARAYYRYDYYAMDY	6		
	V_H2-D_H1-1-J_H4	ARDYYYGSSYYAMDY	2		
	V_H7-D_H1-1-J_H2	ARDGNYFDY	4		
	V_H7-D_H2-J_H2	ARDGNYYFDY	2		
Peritoneal PtC$^+$ aged				347	248 (71%)
	V_H11-D_H1-1-J_H1	MRYGLRYWYFDV	2		
	V_H11-D_H1-1-J_H1	MTYGSSWYFDV	6		
	V_H11-D_H1-1-J_H1	MRYGSYWYFDV	2		
	V_H11-D_H1-3-J_H1	MRYSGYWYFDV	2		
	V_H11-D_H2-J_H1	**MRYGNYWYFDV**	**33**		
	V_H11-D_H1-1-J_H1	MRYSSYWYFDV	17		
	V_H11-D_H1-1-J_H1	MRYGSSYWYFDV	2		
	V_H11-D_H2-J_H1	MRYNGNYWYFDV	2		
	V_H11-D_H1-1-J_H1	MRYGLRYWYFDV	8		
	V_H11-D_H1-3-J_H1	MRYNYRTWYFDV	2		
	V_H12-D_H2-J_H1	AGDRDGYAYFDY	15		
	V_H12-D_H3-J_H1	AGDRSGYWYFDV	5		
	V_H12-D_H1-1-J_H1	AGDSYGYWYFDV	14		
	V_H12-D_H4-J_H1	AGDRLGYWYFDV	2		
	V_H12-D_H2-J_H1	AGDRDGYWYFDV	6		
	V_H12-D_H1-1-J_H1	AGDRYGYWYFDV	20		
	V_H12-D_H1-1-J_H1	AGDYYGYWYFDV	10		
	V_H12-D_H4-J_H1	AGDRWGYWYFDV	25		
	V_H2-D_H2-J_H2	ARPYGNYAHFDY	2		
	V_H2-D_H2-J_H1	ARNPYYGNYYWYFDV	2		
	V_H2-D_H1-1-J_H4	AKIYYYGSSYAMDY	3		
	V_H2-D_H1-2-J_H4	AKIHYYGYYAMDY	3		
	V_H2-D_H4-J_H4	AKTNWDVYYYAMDY	2		
	V_H2-D_H1-1-J_H2	ARVYYYGSSYYFDY	2		
	V_H2-D_H4-J_H4	ARDWDYYAMDY	2		
	V_H2-D_H1-1-J_H4	ARDYGSSYYAMDY	3		
	V_H2-D_H1-1-J_H4	ARDYYGSYYAMDY	3		
	V_H2-D_H1-1-J_H4	ARDYYGSSYYAMDY	10		
	V_H2-D_H1-1-J_H1	ARGYYGSSYWYFDV	3		
	V_H2-D_H1-1-J_H1	ARDYYGSSYWYFDV	20		
	V_H2-D_H1-1-J_H4	ARDIYYGSSYYAMDY	8		
	V_H3-D_H1-1-J_H1	ARDPSYYYGSSYWYFDV	2		
	V_H7-D_H1-1-J_H2	ARDGNYFDY	7		
	V_H7-D_H2-J_H2	ARDGNYYFDY	3		
Peritoneal PtC young				120	24 (20%)
	V_H1-D_H2-J_H4	ARYDGYYAMDY	2		
	V_H1-D_H2-J_H3	ARTRGGYYWFAY	2		
	V_H10-D_H4-J_H3	VAWAY	2		
	V_H11-D_H2-J_H1	MRYDGYYWYFDV	2		
	V_H2-D_H2-J_H4	ARGGWLLHTSYYAMDY	2		
	V_H2-D_H2-J_H4	ASFYDGYYYYYAMDY	2		
	V_H2-D_H1-2-J_H4	ARDRYYGYLYYAMDY	2		
	V_H3-D_H2-J_H3	ATMITTWFAY	2		
	V_H3-D_H2-J_H1	ASGYDWYFDV	3		
	V_H5-D_H1-1-J_H2	ARHYYGSSYYFDY	3		
	V_H7-D_H1-1-J_H2	ARDGNYFDY	2		
Peritoneal PtC$^-$ aged				161	31 (36%)
	V_H1-D_H4-J_H4	ATGTYYAMDY	2		
	V_H1-D_H1-1-J_H3	ARGLNYYGSIPFAY	2		
	V_H11-D_H2-J_H1	MRYDGYYWYFDV	4		
	V_H12-D_H1-1-J_H1	AGDRYGYWYFDV	2		
	V_H1-D_H6-2-J_H4	TRGLWAHAMDY	3		
	V_H2-D_H2-J_H1	ARDYGNYWYFDV	2		

(*Table continues*)

Table I. (*Continued*)

Sample	V-D-J	CDR-H3	Total No. of Sequences with CDR-H3	Total No. of Unique Sequences[a]	Total No. of Replicate Sequences[b]
	V_H3-D_H2-J_H4	AYYDYDYYAMDY	2		
	V_H3-D_H1-1-J_H2	ARRYYGSSYYFDY	2		
	V_H3-D_H2-J_H2	ARYDYDYFDY	2		
	V_H3-D_H1-1-J_H1	YYGSSYWYFDV	4		
	V_H3-D_H1-1-J_H4	ARWDYYGSSYYYAMDY	6		

Replicate sequences are defined as sequences with the exact same V_H, D_H, J_H, N-additions, P-insertions, and subsequent CDR-H3 amino acid sequence. Bolded CDR-H3 indicates the specific CDR-H3 identified by two groups (38, 39) as being utilized frequently in B-1a cells.

[a]The total number of unique sequences within the indicated population.

[b]The total number of replicate sequences with the indicated population.

different population dynamics with age depending upon specificity.

Germline-like structure and repertoire of IgM from splenic PtC-binding B-1a cells changes with age

The largest percent of PtC-binding B-1a cells are found in the peritoneal cavity; however, a small percent of splenic B-1a cells have been shown to bind PtC (43). Because peritoneal PtC^+ B-1a cells keep their germline Ig nature with age (Fig. 1), we asked whether this was also true for PtC^+ B-1a cells found in the spleen. Fig. 3A displays a representative gating strategy. Fig. 3B demonstrates the average percent of splenic B-1a cells binding PtC liposomes increases in aged mice (mean of 4.9% ± 0.84 SEM in young versus 10.3% ± 2.3 SEM in aged mice, $p = 0.0465$). Next, we evaluated the sequence of IgM from PtC-binding (PtC^+) and PtC-nonbinding (PtC^-) splenic B-1a cells in young (3-mo-old) and aged (16- to 23-mo-old) BALB/c-ByJ mice by single-cell PCR. In contrast to peritoneal cavity PtC^+ B-1a cells, we found a significant increase in N-addition with age in IgM derived from splenic PtC^+ B-1a cells. Fig. 3C shows 57% of sequences from splenic PtC^+ B-1a cells in young mice lack N-additions, whereas 46% of sequences from splenic PtC^+ B-1a cells in aged mice lack N-additions ($p = 0.0008$, χ^2, 2×4). We did not observe a significant increase in N-addition with age in IgM derived from splenic PtC^- B-1a cells. Fig. 3C shows 38% of sequences from splenic PtC^- B-1a cells in young mice lack N-additions, whereas 35% of sequences from splenic PtC^- B-1a cells in aged mice lack N-additions. Examining the junctions independently (Fig. 3D) in the splenic PtC^+ B-1a cells reveals increased N-addition length at both junctions and the sum of the two junctions; however, only at the D-J and sum of the two junctions does this increase reach statistical significance (D-J: young mean length = 0.61 ± 0.13 SEM versus aged mean length = 1.10 ± 0.11 SEM, $p = 0.0004$; sum of the two junctions: young mean length = 1.88 ± 0.28 SEM versus aged mean length = 2.60 ± 0.23 SEM, $p = 0.0287$). No significant differences are observed in the splenic PtC^- B-1a cells when examining the junctions independently (Fig. 2D). Together, these results are different from peritoneal PtC^+ B-1a cells, as splenic PtC^+ B-1a cell IgM moves away from the germline with increasing age; however, splenic PtC^- B-1a cell IgM does not change in germline status with age.

V_H, D_H, and J_H analysis reveals differences between young and aged splenic PtC^+ B-1a cells (Fig. 4). Interestingly, splenic PtC^+ B-1a cells from young mice use V_H11 more frequently than splenic PtC^+ B-1a cells from aged mice (40% in young versus 25% in aged mice, $p < 0.0041$). Furthermore, we observe splenic PtC^- B-1a cells from aged mice use V_H11 and V_H14 more frequently than splenic PtC^- B-1a cells from young mice (V_H11 = 6% in aged versus 1% in young mice, $p = 0.0368$; V_H14 = 11% in aged versus 3% in young mice, $p = 0.0097$). These results are shown in Fig. 4A.

The splenic PtC^+ B-1a cells contained a number of replicate sequences (Fig. 4B, Table II) although at a lower frequency than observed in peritoneal PtC^+ B-1a cells (Table I). Within the replicate sequences of splenic PtC^+ B-1a cells, we observe diversity in L chain use (Supplemental Fig. 1B) similar to peritoneal PtC^+ B-1a cells (Supplemental Fig. 1A). Of the 124 total sequences from young PtC^+ splenic B-1a cells, 56 were replicate sequences (45%). Of the 222 total sequences from aged splenic PtC^+ B-1a cells, 86 were replicate sequences (39%). As seen in the peritoneal cavity PtC^+ B-1a cells, V_H11 and V_H12 make up most of the replicates in the splenic PtC^+ B-1a cells (Fig. 4B, Table II). Interestingly, the aged splenic PtC^+ population has a greater diversity within the replicate sequences (Fig. 4C); however, this diversity is less than in the aged peritoneal cavity PtC^+ B-1a cells (Fig. 2C). The CDR-H3 amino acid sequence MRYGNYWYFDV shown to be prevalent in the peritoneal B-1a cell population by others (38, 39) and in our results in this article (Table I) is also present within the splenic PtC^+ B-1a cell population (Table II, CDR-H3 in bold type). Comparing sequences we obtained from splenic PC^+ B-1a cells versus splenic PtC^+ B-1a cells, we found a few identical CDR-H3 sequences shared between PC- and PtC-specific peritoneal B-1a cells in the young and aged mice (Supplemental Fig. 2B). These results demonstrate of all PC and PtC sequences there are 0.9% identical CDR-H3 amino acid sequences shared between PC- and PtC-specific B-1a cells in the young, whereas 0.6% are shared between the aged populations of PC and PtC B-1a cells. The prominent MRYGNYWYFDV sequence was found in both PC- and PtC-specific B-1a cell populations in the aged mice (Supplemental Fig. 2B). Unlike peritoneal PtC^+ B-1a cells, the overall frequency of this specific CDR-H3 increases in the aged mice (10% in young and 13% in aged). Again, these data indicate an age-associated skewing of this specificity, which could have implications pertaining to how protective Abs are selected and maintained with age.

Examination of the D_H and J_H genes shows significant differences in utilization in the aged versus young splenic PtC populations. Splenic PtC^+ B-1a cells from aged mice use D_H4 more frequently than young mice (8% in aged versus 2% in young mice, $p = 0.0453$), whereas splenic PtC^+ B-1a cells from young mice use DFL16.1 more frequently than aged mice (52% in aged versus 39% in young mice, $p = 0.0255$) (Fig. 4D). Similarly in the splenic PtC^- B-1a cell population, the aged mice use D_H4 more frequently and DFL16.1 less frequently than young mice (D_H4 = 17% in aged versus 5% in young mice, $p = 0.0029$; DFL16.1 = 20% in aged versus 34% in young mice, $p = 0.0054$) (Fig. 4D). In terms of J_H usage (Fig. 4E), splenic PtC^+ B-1a cells from aged mice use J_H3 more frequently than young mice (19% in aged versus 9% in young mice, $p = 0.0099$). In splenic PtC^- B-1a cells, J_H3 is used more frequently and J_H4 less frequently in aged mice as compared with young (J_H3 = 24% in aged versus 12% in young

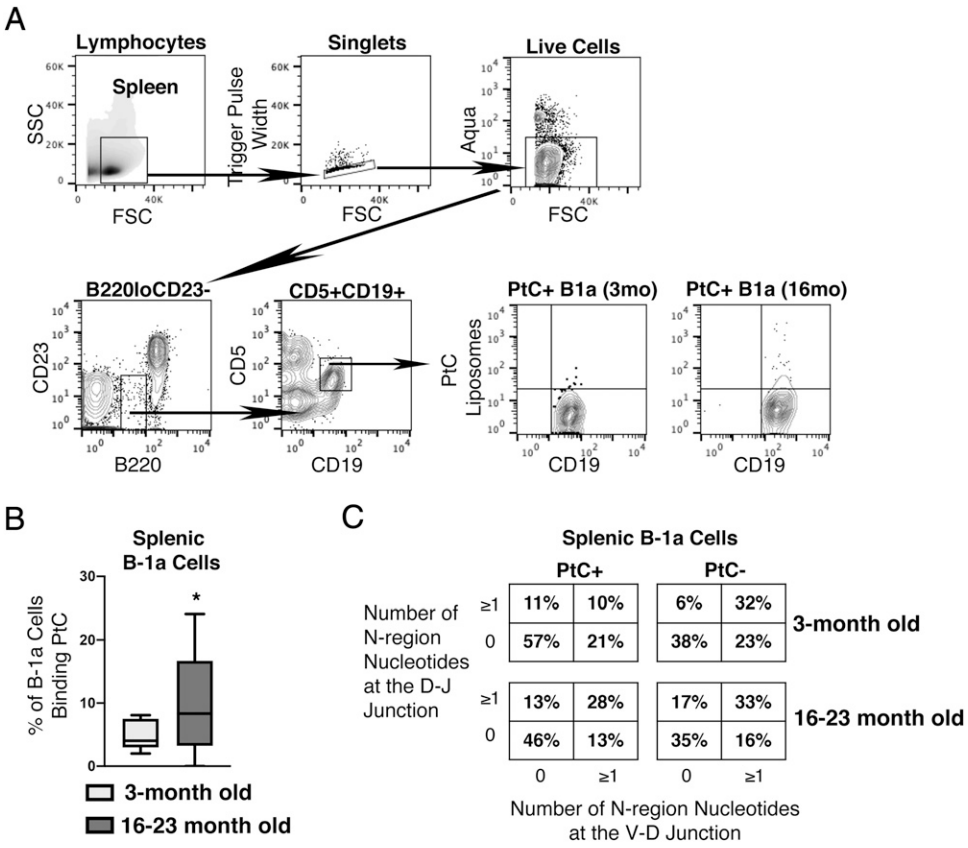

D

B1a Cell Population	V-D (nt)	D-J (nt)	Sum (nt)	Number of Sequences
Spleen PtC+ Young	1.27	0.61	1.88	n = 124
Spleen PtC+ Aged	1.50	1.10	2.60	n = 222
Spleen PtC- Young	2.40	1.30	3.70	n = 111
Spleen PtC- Aged	1.70	1.50	3.20	n = 209

FIGURE 3. Splenic PtC$^+$ and PtC$^-$ B-1a cell IgM differ in germline status in aged mice. Splenocytes were obtained from 3- to 23-mo-old BALB/c-ByJ male mice and analyzed for PtC$^+$ and PtC$^-$ B-1a cells by immunofluorescent staining. (**A**) Representative gating strategy for analysis and sorting of splenic PtC$^+$ B-1a cells. (**B**) Average percent of splenic B-1a cells binding PtC liposomes (±SEM). (**C** and **D**) PtC$^+$ and PtC$^-$ B-1a cells were single-cell sorted from 3- and 16- to 23-mo-old (as indicated) male BALB/c-ByJ mice. The V_H region was amplified and sequenced as detailed in *Materials and Methods*. (C) The percent of sequences with zero N-additions at both junctions, one or more N-additions at both junctions, zero N-additions at V-D and one or more at D-J junctions, or zero N-additions at D-J and one or more at V-D junctions is shown. (D) Average number of N-additions at the V-D, D-J, or sum of the two junctions. Results are based on three independent experiments with sequences from 3-mo-old mice (n = 5) and 16- to 23-mo-old mice (n = 7). Statistics used: (B and D) Mann–Whitney U test and (C) 2 × 4 χ^2 test. *$p \leq 0.05$ (exact p values are defined in the text).

mice, p = 0.0089; J_H4 = 29% in aged versus 42% in young, p = 0.0139). These results demonstrate PtC$^+$ B-1a cells in the spleen undergo similar selective pressures over time as the total and PC-specific peritoneal B-1a cell populations (33) yet different from peritoneal PtC$^+$ B-1a cells (Fig. 1).

Structure and repertoire of IgM from total splenic B-1a cells does not change with age

Recent studies have analyzed the repertoire of the total splenic B-1a cell population in young mice and found these B-1a cells have a larger number of N-additions as compared with peritoneal B-1a cells (38, 44). In this study, we observe a similar finding with splenic PtC$^-$ B-1a cell IgM containing a larger number of N-additions in the young (38% lacking all N-additions [Fig. 3C]) as compared with IgM from the young peritoneal PtC$^-$ B-1a cell population (58% lacking all N-additions [Fig. 1C]) (p = 0.0384, χ^2, 2 × 4). Interestingly, we did not observe a significant change in N-additions with age in the splenic PtC$^-$ B-1a cell population (Fig. 3C), which we observed in the peritoneal PtC$^-$ B-1a cell population (Fig. 1C). Therefore, we asked whether the total splenic B-1a cell population changes with increased age. In fact, we found no change in the number of sequences with zero N region additions at both junctions in young (31%) versus aged (32%) total splenic B-1a cells (Fig. 5A). Replicate sequences were also observed in the total splenic B-1a cell population (9% in young and 18% in the aged mice) (Table II). There was no significant difference in the number of sequences with zero N region additions at both junctions in young (29%) versus aged (31%)

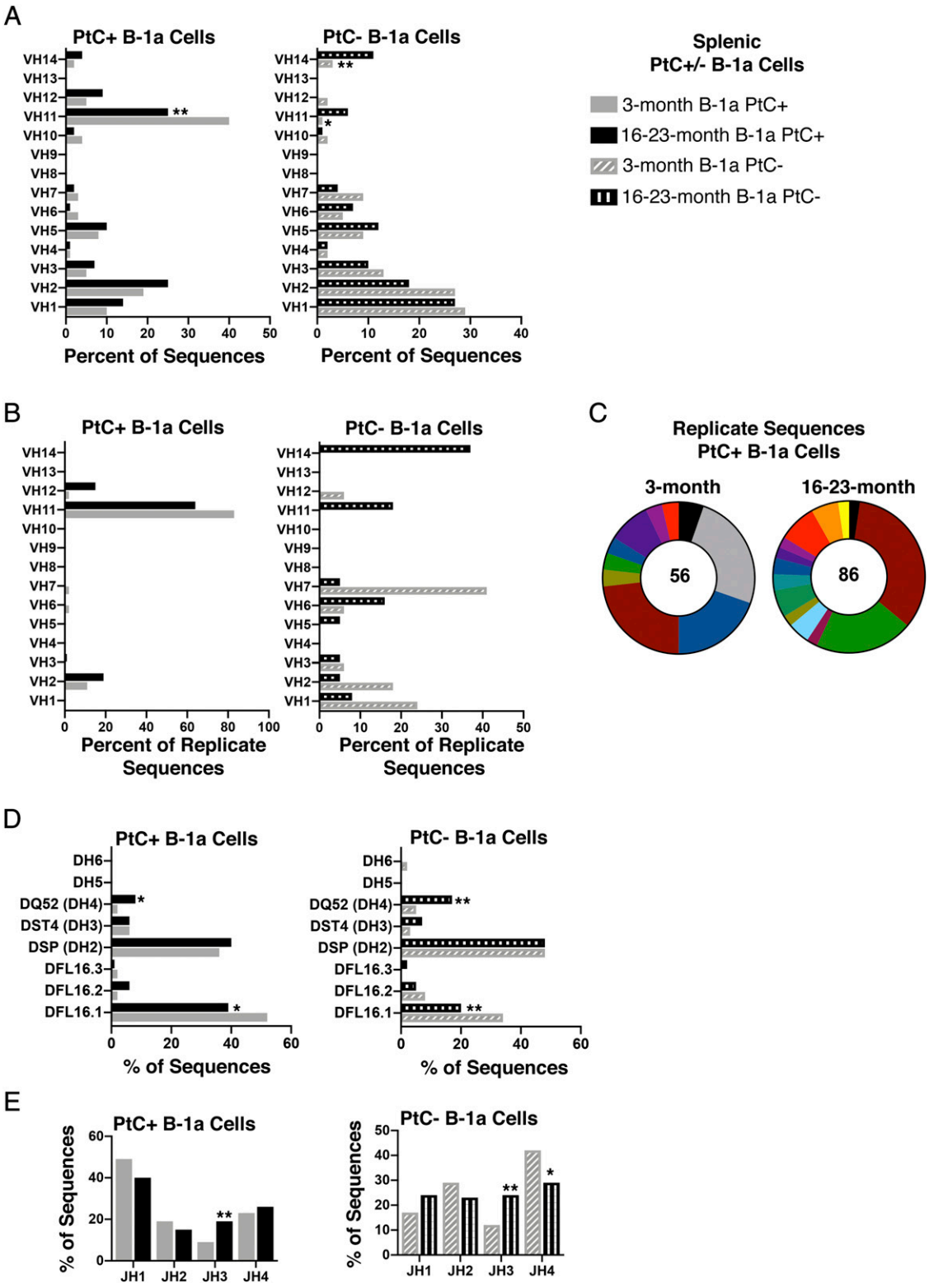

FIGURE 4. Repertoire analysis of natural IgM from splenic PtC$^+$ and PtC$^-$ B-1a cells in aged and young adult mice. Splenic PtC$^+$ B-1a cells were single-cell sorted from 3-to 23-mo-old (as indicated) male BALB/c-ByJ mice. The V_H region was amplified and sequenced as detailed in *Materials and Methods*. (**A**) The percent of V_H gene segment usage. (**B**) The percent of V_H gene segment usage within the replicate sequences is displayed. (**C**) Distribution of replicate CDR-H3 sequences in the young and aged mice (number in the middle represents the number of replicates within the population). Each color represents a unique CDR-H3 amino acid sequence. (**D**) The percent of D_H gene segment usage. (**E**) The percent of J_H gene segment usage. Results are based on three independent experiments with sequences from 3-mo-old mice ($n = 5$) and 16- to 23-mo-old mice ($n = 7$). Statistics used: 2×2 χ^2 test. $^*p \leq 0.05$, $^{**}p \leq 0.01$ (exact p values are defined in the text).

Table II. Replicate sequences within splenic PtC$^+$ and PtC$^-$ B-1a cells

Sample	V-D-J	CDR-H3	Total No. of Sequences with CDR-H3	Total No. of Sequences[a]	Total No. of Replicate Sequences[b]
Splenic PtC$^+$ young				124	56 (45%)
	V_H11-D_H2-10-J_H1	TSYGNYWYFDV	3		
	V_H11-D_H1-1-J_H1	MRYGGYWYFDV	14		
	V_H11-D_H1-1-J_H1	MRYGSYWYFDV	11		
	V_H11-D_H2-1-J_H1	**MRYGNYWYFDV**	**13**		
	V_H11-D_H1-1-J_H1	MRYGPYWYFDV	2		
	V_H12-D_H1-1-J_H2	AGDRWGYGSFDY	2		
	V_H2-D_H1-1-J_H1	ARDYYGSSYWYFDV	2		
	V_H2-D_H2-14-J_H4	ARAYYRYDYYAMDY	5		
	V_H6-D_H2-3-J_H1	IHYDGYYWYFDV	2		
	V_H7-D_H1-1-J_H2	ARDGNYFDY	2		
Splenic PtC$^+$ aged				222	86 (39%)
	V_H11-D_H1-1-J_H1	MRYGPYWYFDV	2		
	V_H11-D_H2-1-J_H1	**MRYGNYWYFDV**	**29**		
	V_H11-D_H1-1-J_H1	MRYGSSYWYFDV	18		
	V_H12-D_H4-J_H1	AGDSTGYWYFDV	2		
	V_H12-D_H3-J_H1	AGDRSGYWYFDV	4		
	V_H12-D_H4-J_H1	AGDRLGYWYFDV	2		
	V_H12-D_H1-1-J_H1	AGDYYGYWYFDV	5		
	V_H12-D_H4-J_H1	AGDRWGYWYFDV	3		
	V_H2-D_H1-1-J_H2	ARVYYYGSSYYFDY	3		
	V_H2-D_H1-1-J_H2	ARTYYYGSSYYFDY	2		
	V_H2-D_H1-2-J_H4	ARDYYGYVYAMDY	2		
	V_H2-D_H1-1-J_H4	ARYYYGSSYYYAMDY	7		
	V_H2-D_H2-4-J_H4	ARDRRTMITTDYAMDY	5		
	V_H3-D_H1-1-J_H4	ARSLYYYGSSYAMDY	2		
Splenic PtC$^-$ young				111	25 (23%)
	V_H1-D_H1-1-J_H4	ARDPSYYYGSSYGAMDY	2		
	V_H1-D_H2-4-J_H1	ARDYDYWYFDV	2		
	V_H1-D_H1-1-J_H1	ARSYYGSSYWYFDV	3		
	V_H2-D_H1-1-J_H1	AKYGSSYWYFDV	2		
	V_H2-D_H2-13-J_H1	ARGGGTWYFDV	2		
	V_H2-D_H2-14-J_H4	ARDKSYRYDLYYYAMDY	2		
	V_H3-D_H2-4-J_H2	ARWGYDYEAYFDY	2		
	V_H6-D_H2-4-J_H2	TIYYDYDYFDY	2		
	V_H7-D_H1-1-J_H2	ARDGNYFDY	8		
Splenic PtC$^-$ aged				209	50 (24%)
	V_H11-D_H2-1-J_H1	MRYNGNYWYFDV	4		
	V_H11-D_H2-3-J_H1	MRYDGYYWYFDV	5		
	V_H14-D_H4-J_H1	ANWDWYFDV	12		
	V_H14-D_H4-J_H1	ARWDWYFDV	4		
	V_H1-D_H4-J_H3	ARSNHAWFAY	4		
	V_H2-D_H2-14-J_H4	AHLYYRYDPYAMDY	2		
	V_H2-D_H4-J_H4	ASNIYYAMDY	2		
	V_H3-D_H2-4-J_H4	ARYYDYDYYAMDY	2		
	V_H3-D_H2-12-J_H4	AYDYAMDY	2		
	V_H5-D_H1-1-J_H2	ARHYYGSSYYFDY	3		
	V_H6-D_H4-J_H3	TNWDAY	7		
	V_H7-D_H2-1-J_H2	ARDGNYYFDY	3		
Splenic B-1a young				210	18 (9%)
	V_H1-D_H1-1-J_H2	ARYYYGSSYFDY	3		
	V_H11-D_H1-1-J_H1	MRYGSYWYFDV	2		
	V_H11-D_H2-J_H1	**MRYGNYWYFDV**	**7**		
	V_H2-D_H2-J_H4	AKENPGYYLYYYAMDY	2		
	V_H2-D_H1-1-J_H1	AGEYGFPLITTVVGGTSM	2		
	V_H2-D_H1-1-J_H1	ARDYYGSSYWYFDV	2		
	V_H2-D_H2-J_H4	ARVWFLPPYYAMDY	2		
	V_H2-D_H2-J_H4	ARDRGYYGNYVLYSYYAMDY	2		
	V_H3-D_H2-J_H4	AEYGNYDYAMDY	2		
	V_H6-D_H2-J_H2	TRYGNYYFDY	3		
Splenic B-1a aged				148	27 (18%)
	V_H1-D_H1-1-J_H2	ARWYYFDY	2		
	V_H1-D_H2-J_H2	ARGYDYDFDY	7		
	V_H11-D_H1-1-J_H1	MRYGLRYWYFDV	2		
	V_H14-D_H4-J_H1	ARWDWYFDV	2		
	V_H2-D_H2-J_H3	AREGDGYYSLFAY	2		
	V_H3-D_H2-J_H4	ARELDY	2		
	V_H3-D_H2-J_H2	ARYYGNYFDY	2		
	V_H5-D_H1-1-J_H2	ARHYYGSSYYFDY	2		
	V_H6-D_H1-1-J_H4	TRYGYAMDY	2		

Replicate sequences are defined as sequences with the exact same V_H, D_H, J_H, N-additions, P-insertions, and subsequent CDR-H3 amino acid sequence. Bolded CDR-H3 indicates the specific CDR-H3 identified by two groups (38, 39) as being utilized frequently in B-1a cells.

[a]The total number of unique sequences within the indicated population.

[b]The total number of replicate sequences with the indicated population.

total splenic B-1a cells when only one representative replicate is analyzed (Fig. 5B, without replicates). Therefore, we continue the analysis including replicates. The findings observed in Fig. 5A are further reflected in the N-addition length at both junctions, which shows no significant difference in N-addition length between young and aged mice at the V-D, D-J, or sum of the two junctions (Fig. 5C). Analysis of V_H gene usage showed a significant decrease in V_H2 use in aged splenic B-1a cells (28% in young versus 18% in aged mice, $p = 0.0212$) (Fig. 5C). Examination of D_H and J_H usage in the splenic B-1a cell population revealed no significant differences between young and aged mice (Fig. 5D, 5E). Together these results demonstrate IgM from the total splenic B-1a cell population in the young displays more N-additions (less germline IgM) than IgM from total peritoneal B-1a cells, which is in line with previously published studies (38, 44). However, unlike the aged peritoneal B-1a cell population, aged splenic B-1a cells and aged splenic PtC B-1a cells do not move further away from the germline as evidenced by no change in N-additions in aged mice.

Number of PtC$^+$ peritoneal and splenic B-1a cells in the aged mice

Our results demonstrating an increase in the percent of B-1a cells that bind PtC in the spleen with age (Fig. 3B) suggest an increase in the total number of splenic PtC$^+$ B-1a cells in aged mice. As shown in Fig. 6, the percent of B-1a cells in the spleen (Fig. 6A, $p = 0.0083$), total number of splenic B-1a (Fig. 6B, $p < 0.0001$), and the total number of splenic PtC$^+$ B-1a cells (Fig. 6C, $p = 0.0381$) are all significantly lower in the aged mice. Despite the percent of splenic PtC$^+$ B-1a cells increasing with age, the actual number of splenic PtC$^+$ B-1a cells was significantly lower in aged mice as compared with young because the total percent of splenic B-1a cells was diminished in aged mice. The percent of peritoneal B-1a (Fig. 6D, $p < 0.0001$) and total number of peritoneal B-1a cells (Fig. 6E, $p = 0.0155$) are also significantly lower in aged mice; however, the decline was not as great as in the spleen, and thus there is no significant difference in the total number of peritoneal PtC$^+$ B-1a cells with age (Fig. 6F). These results showing a significant decline in splenic and peritoneal B-1a cell numbers in aged male BALB/c-ByJ mice are consistent with what has been shown for human B1 cells in people over the age of 65 (45). Because splenic B-1a cells contribute directly to serum IgM levels, our results suggest a decline in serum levels of PtC-specific Ab. To test this, we analyzed serum from young and aged mice for the levels of DMPC- and DOPC-specific IgM (Fig. 6G). Interestingly, we observed significantly more DMPC- and DOPC-specific IgM in serum from aged mice ($p < 0.0001$ and $p = 0.0039$, respectively). It should be noted that at this time, we do not know if the IgM binding to the DMPC coated on the ELISA strips is similar to the PtC Ag in the liposomes; therefore, the ELISA results may not directly correspond to serum titers of PtC-specific IgM measured by liposomes. Even so, these results are in line with a possible increase in PtC Ag in the aged mice because of an increase in damaged or senescent RBCs. However, the decrease in the number of splenic PtC$^+$ B-1a cells would disfavor the increase we observe in the serum of aged mice. Therefore, we examined the ability of aged splenic (B-1aS) and peritoneal B-1a cells (B-1a) to secrete IgM by ELISPOT. We found an increase in the percent of splenic B-1a cells secreting IgM (Fig. 6H) as well as an increase in spot size (Fig. 6I). Although these results did not reach a level of significance, they suggest an increase in the number of secreting cells, and an increase in amount of secretion per cell could account for the increase in PtC-specific IgM we observe in the serum of aged mice. We have previously observed no change in PPS3-specific IgM or PC-specific IgM at 18 mo of age; however, we did observe significantly lower levels of PC-specific IgM at 23–24 mo of age (33). Together, these results demonstrate a decrease in peritoneal and splenic B-1a cells in aged male mice. Furthermore, whereas the number of splenic PtC B-1a cell decreases with age, the amount of serum PtC-specific IgM increases with age, which could be due to an increase in the number of splenic B-1a cells secreting Abs in aged mice.

Germline status of V_H11, V_H12, V_H2, and accompanying D_H and J_H use in peritoneal and splenic PtC-binding B-1a cells changes with age

Because we observed a significant difference in the number of N-additions in the aged peritoneal PtC$^+$ B-1a cell population (63% zero N-additions at both at junctions) as compared with the aged splenic PtC$^+$ B-1a cell population (46% zero N-additions at both junctions), we examined the number of N-additions within PtC$^+$ B-1a cells utilizing V_H11, V_H12, or V_H2 (Table III). In all populations of PtC$^+$ B-1a cells using V_H11 or V_H12, the number of N-additions at both junctions remained low in the aged populations (Table III). This is in line with Hardy and colleagues' (30) work, demonstrating recombinations involving V_H11 do not tolerate N-additions. In contrast, an increase in N-additions was observed with age in splenic PtC$^+$ B-1a cells using V_H2 (Table III). Overall, these data demonstrate minimal changes in the number of N-additions in cells using V_H11 regardless of the location or age of the PtC$^+$ B-1a cells.

Studies by Herzenberg and colleagues (42, 46) have shown PtC-binding peritoneal B-1a cells from BALB/c mice use V_H2 (Q52) most frequently; however, the BALB/c strain also produces anti-PtC Abs using V_H11 and V_H12, just at a lower frequency. In light of these previous studies, we examined whether these observations hold true in aged PtC$^+$ B-1a cells from the peritoneal cavity and spleen. The young peritoneal PtC$^+$ B-1a cell data presented in this study (55%, Fig. 2A) reflect the previous finding of preferential V_H2 usage in BALB/c mice (46); however, our data further show that in aged BALB/c-ByJ mice, peritoneal PtC$^+$ B-1a cells use V_H2 (31%), V_H11 (24%), and V_H12 (31%) at similar frequencies (Fig. 2A, Supplemental Fig. 3A). In contrast, splenic PtC$^+$ B-1a cells from young BALB/c-ByJ mice used V_H11 (40%) most frequently (Fig. 4A, Supplemental Fig. 3A). This V_H11 use in young splenic PtC$^+$ B-1a cells changed with age to V_H11 (25%), V_H2 (25%), and V_H12 (9%) (Fig. 4A, Supplemental Fig. 3A).

Previous studies have shown peritoneal PtC$^+$ B-1a cells from BALB/c mice have preferential use of D_H and J_H genes depending upon the V_H used (42, 46). These studies demonstrated the following in PtC$^+$ B-1a cells: 1) V_H11 preferentially use D_H2 and J_H1, 2) V_H12 preferentially use $D_H16.1/D_H2$ and J_H1, and 3) V_H2 preferentially use $D_H16.1/D_H2$ and J_H4. These observations are also seen in our data for young peritoneal PtC$^+$ B-1a cells (Supplemental Fig. 3B, 3C). In general, our data demonstrate aged peritoneal PtC$^+$ B-1a cells using V_H11 increase DFL16.1 use, whereas aged splenic PtC$^+$ B-1a cells increase D_H2 use (Supplemental Fig. 3). Aged peritoneal and splenic PtC$^+$ B-1a cells using V_H12 increase D_H4 usage. Young and aged splenic PtC$^+$ B-1a cells using V_H2 increase J_H3 use (Supplemental Fig. 3). Together, these results demonstrate 1) differences in V_H and D_H use of PtC$^+$ B-1a cells depending on location (spleen versus peritoneal cavity) and with age and 2) minimal differences in J_H usage for peritoneal cavity– or spleen-derived PtC$^+$ B-1a cells using V_H11, V_H12, or V_H2 (Supplemental Fig. 3). Importantly, these results show peritoneal and splenic PtC$^+$ B-1a cells are being selected differently over time depending upon their location.

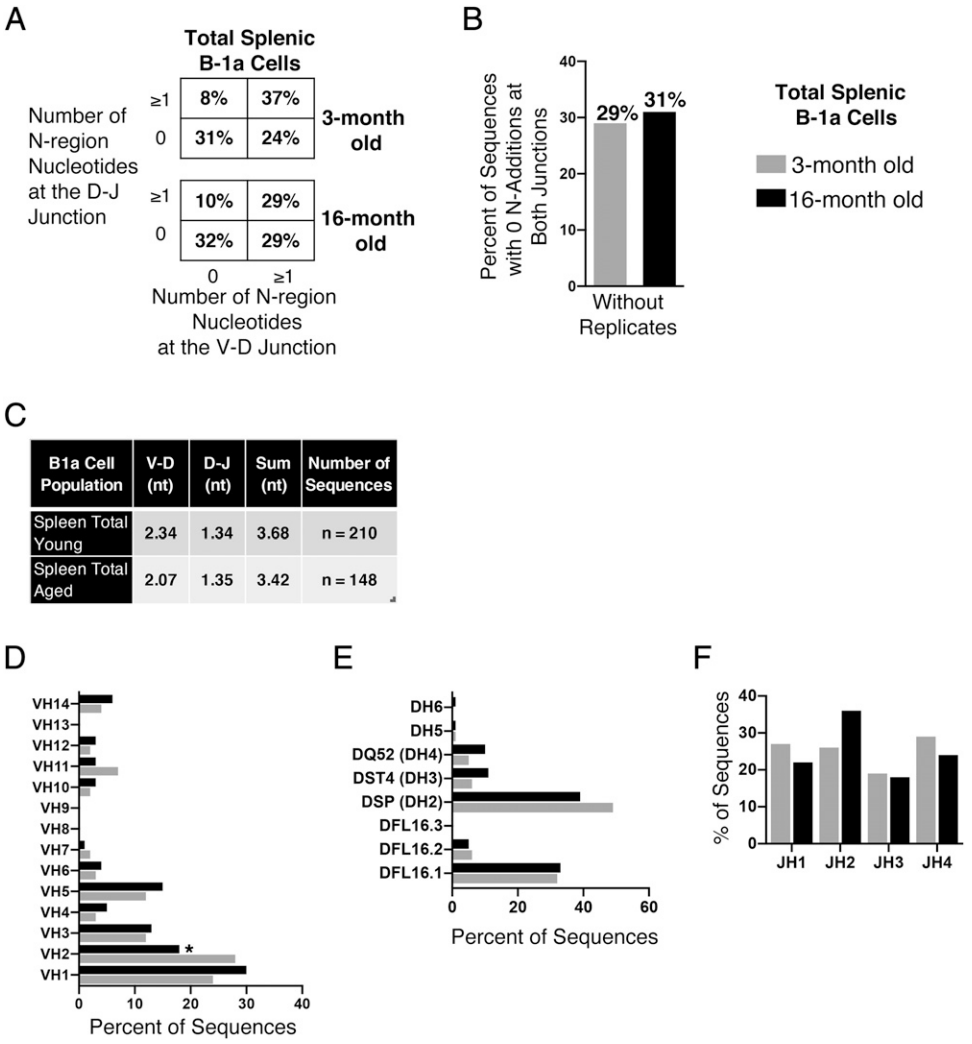

FIGURE 5. Total splenic B-1a cell IgM does not differ in germline status in middle-aged and young mice. Total splenic B-1a cells were single-cell sorted from 3- to 16-mo-old (as indicated) male BALB/c-ByJ mice. The V_H region was amplified and sequenced as detailed in *Materials and Methods*. (**A**) The percent of sequences with zero N-additions at both junctions, one or more N-additions at both junctions, zero N-additions at V-D and one or more at D-J junctions, or zero N-additions at D-J and one or more at V-D junctions is shown. (**B**) The percent of sequences containing zero N-additions at both junctions is shown without replicate sequences included in the analysis. (**C**) Average number of N-additions at the V-D, D-J, or sum of the two junctions. (**D**) The percent of V_H gene segment usage. (**E**) The percent of D_H gene segment usage. (**F**) The percent of J_H gene segment usage. Results are based on two independent experiments with sequences from 3-mo-old mice (n = 3) and 16-mo-old mice (n = 4). Statistics used: (A and B) 2 × 4 χ^2 test, (C) Mann–Whitney U test, and (D–F) 2 × 2 χ^2 test.

Germline-like structure and repertoire of IgM from splenic PC-binding B-1a cells changes with age

We have previously demonstrated PC-binding (PC^+) peritoneal B-1a cells move away from germline with age (as evidenced by an increase in N-additions) (33). In light of the data presented in this study demonstrating differences in germline status of PtC^+ B-1a cells is dependent upon location (peritoneal cavity versus spleen), we assessed the structure of IgM from PC^+ splenic B-1a cells. As shown in Fig. 7A, splenic PC^+ B-1a cells from middle-aged (11- to 16-mo-old) mice produce IgM with more N-additions at both junctions (15% of sequences lack N-additions at both junctions) as compared with young (3-mo-old) mice (38% of sequences lack N-additions at both junctions) (χ^2, 2 × 4, $p = 0.0011$). In line with the increase in N-additions at both junctions in the aged mice, there is a significant increase in the length of N-additions in aged mice at the V-D junction ($p < 0.0001$), D-J junction ($p = 0.0021$), and at the sum of the two junctions ($p < 0.0001$) (Fig. 7B). Analysis of V_H and D_H usage did not reveal any statistically significant differences in splenic PC^+ B-1a cell IgM from 11- to 16-mo-old mice versus 3-mo-old mice (Fig. 7C, 7D). There were significant differences in J_H1, J_H2, and J_H4 usage between the aged (10, 38, and 29%, respectively) and young splenic PC^+ B-1a cells (20, 21, and 43%, respectively) (Fig. 7E). As with peritoneal B-1a cells that bind PC, splenic PC^+ B-1a cells also change with age in that the IgM they produce contains more N-additions. Such a change away from germline would leave the individual with IgM that is less protective against pneumococcal infection as previously shown (29).

Hydrophobicity and amino acid composition of the CDR-H3 loop changes with age and V_H usage

Abs have six CDRs. CDR-H3 is the central point for Ag contact and the most variable. Therefore, the properties of the amino acids comprising the CDR-H3 have the most influence on Ag interaction with Ab. Elegant studies have shown the CDR-H3 of autoreactive Abs is more charged than the CDR-H3 of non-autoreactive Abs (41, 47). Because we identified differences with age of peritoneal or splenic B-1a cells bearing different specificities, we examined the

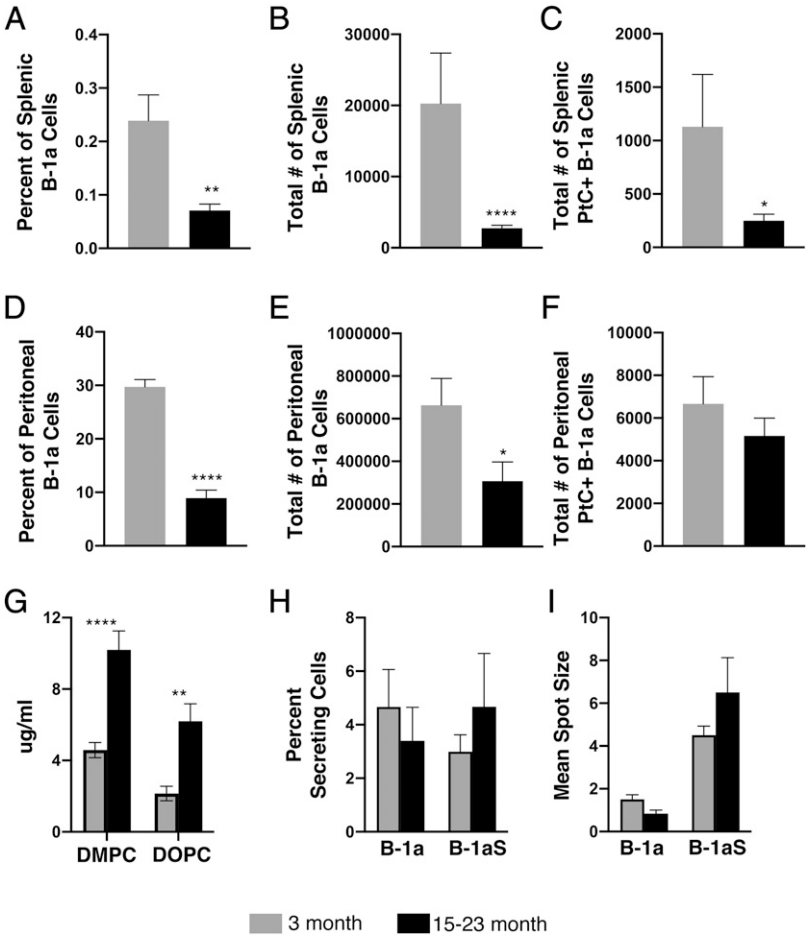

FIGURE 6. The number of B-1a cells differs in aged mice. B-1a cells examined in the young and aged mice were assessed for percent and number. (**A**) The percent of live splenocytes staining positive for B-1a cells ($B220^{lo}CD5^{+}CD19^{hi}CD23^{-}$), (**B**) total number of splenic B-1a cells, and (**C**) the total number of splenic PtC^{+} B-1a cells in young (gray, $n = 9$) or aged (black, $n = 11$) mice. (**D**) The percent of live peritoneal lymphocytes staining positive for B-1a cells ($B220^{lo}CD5^{+}CD19^{hi}CD23^{-}$), (**E**) total number of peritoneal B-1a cells, and (**F**) the total number of peritoneal PtC^{+} B-1a cells in young (gray, $n = 14$) or aged (black, $n = 17$) mice. (**G**) The amount of anti-DMPC or anti-DOPC IgM in the serum of young (gray, $n = 10$) or aged (black, $n = 10$) mice (relative to NC-17 Ab), as measured by ELISA. (**H**) The percent of peritoneal B-1a (B-1a) or splenic B-1a (B-1aS) cells secreting Ab was measured by ELISPOT in young (gray, $n = 6$) and aged (black, $n = 6$) mice. (**I**) The mean spot size of peritoneal B-1a (B-1a) or splenic B-1a (B-1aS) cells secreting Ab was measured by ELISPOT in young (gray, $n = 6$) and aged (black, $n = 6$) mice. Results are based on four independent experiments. Statistics used: Mann–Whitney U test. $*p \leq 0.05$, $**p \leq 0.01$, $****p \leq 0.0001$ (exact p values are defined in the text).

hydrophobicity of these B-1a cell populations to determine if there are significant changes within the CDR-H3 region. Using the Kyte-Doolittle scale, we calculated the average hydrophobicity of each CDR-H3 loop. Our results demonstrate the CDR-H3 loop of peritoneal PtC^{+} B-1a cell IgM increases in charge (decreases in hydrophobicity) with age (-0.017 ± 0.02 in young versus -0.27 ± 0.01 in aged mice, $p = 0.0003$) (Fig. 8A). Such an increase in charge might be predicted in PtC^{+} B-1a cells in the aged mice because PtC is found on damaged or senescent RBCs and such autoantigens increase in the aged mice. Our results showing an increase in serum PtC-specific IgM (Fig. 6G) are in line with an increase of such autoantigens in the aged. There is also a significant change in peritoneal PtC^{-} B-1a cells; however, unlike peritoneal PtC^{+} B-1a cells, the CDR-H3 loop of PtC^{-} B-1a cell IgM decrease in charge with age (-0.16 ± 0.03 in young versus -0.08 ± 0.02 in aged mice, $p < 0.0001$) (Fig. 8A). There were no significant differences in hydrophobicity observed in any of the splenic B-1a cell populations with age (Fig. 8A).

Next, we looked further into the hydrophobicity of PtC-binding B-1a cells using V_H11, V_H12, or V_H2 (Fig. 8B). Interestingly, PtC^{+} B-1a cells using V_H11 and V_H12 are overall slightly more charged than the total B-1a cell populations as seen in Fig. 8A, whereas PtC^{+} B-1a cells using V_H2 are slightly more hydrophilic (Fig. 8B). Peritoneal PtC^{+} B-1a cells expressing V_H11 decrease in charge with age (-0.29 ± 0.010 in young versus -0.25 ± 0.010 in aged mice, $p = 0.0053$). Peritoneal PtC^{+} B-1a cells expressing V_H12 are the most highly charged group and increase in charge with age (-0.29 ± 0.047 in young versus -0.41 ± 0.0084 in aged mice, $p = 0.0038$). Peritoneal PtC^{+} B-1a cells expressing V_H2 similarly increases in charge with age (-0.091 ± 0.021 in young versus -0.16 ± 0.015 in aged mice, $p = 0.0151$). Splenic PtC^{+} B-1a cells expressing V_H12 markedly decrease in charge with age (-0.39 ± 0.034 in young versus -0.13 ± 0.020 in aged mice, $p < 0.0001$), whereas there is little change in the charge of splenic V_H2 and V_H11 Abs with age (Fig. 8B).

The hydrophobicity of the CDR-H3 is highly influenced by D_H usage, J_H usage, N region additions, and/or amino acid content within the CDR-H3 (41). The amino acid content within the CDR-H3 of mature murine B cells shows a predominance of tyrosine and glycine (48, 49). Importantly, changes in the amino acid content of the CDR-H3 have been shown to result in decreased B cell development and Ab production and an increase in susceptibility to infection (50–52). Therefore, we examined the amino acid content of the CDR-H3 regions of these B-1a cell populations (Fig. 9). Comparing the overall amino acid content, there are significant differences (χ^2, df = 19) between young and aged peritoneal PtC^{+} B-1a cells ($p < 0.0001$), peritoneal PtC^{-} B-1a cells ($p < 0.0001$), and splenic PtC^{+} B-1a cells ($p = 0.0282$). Our analysis demonstrates this same predominance of tyrosine and to a lesser extent glycine in all populations of young B-1a cells (Fig. 9), as well as young and aged B-1a cell populations using V_H11 and V_H12 (Fig. 10). Significantly reduced use of tyrosine is seen in aged peritoneal PtC^{-} B-1a (27 versus 36%, $p = 0.0007$), splenic PtC^{+} B-1a (34 versus 40%, $p = 0.0358$), splenic PtC^{-} B-1a (29 versus 36%, $p = 0.0170$), and splenic PC^{+} B-1a (26 versus 33%, $p = 0.0279$) cells as compared with their young counterparts (Fig. 9). Peritoneal PtC^{-} B-1a cells display the most significant changes in amino acid content with age. Aged peritoneal PtC^{-} B-1a cells display a decrease in the percent of glycine in the aged mice (12 versus 8%, $p = 0.0013$), as well as asparagine (4 versus

Table III. Germline status (N-additions) of peritoneal and splenic PtC$^+$ B-1a cells using V_H11, V_H12, or V_H2 variable regions

B-1a Cell Population	Percent of Sequences Lacking N-additions at Both Junctions			
	All V_H	V_H11	V_H12	V_H2
PerC PtC$^+$ B-1a 3 mo	61 (n = 166)	93 (n = 42)	64 (n = 11)	53 (n = 91)
PerC PtC$^+$ B-1a 15–18 mo	63 (n = 347)	73 (n = 82)	76 (n = 108)	52 (n = 109)
Spleen PtC$^+$ B-1a 3 mo	57 (n = 124)	88 (n = 49)	67 (n = 6)	54 (n = 24)
Spleen PtC$^+$ B-1a 16 mo	46 (n = 222)	91 (n = 55)	63 (n = 19)	42 (n = 55)

The numbers indicate the percent of sequences containing zero N-additions a both junctions from the indicated B-1a cell population using V_H11, V_H12, or V_H2.

2%, p = 0.0034), histidine (2 versus 1%, p = 0.0107), and leucine (4 versus 2%, p = 0.0103), whereas these cells display an increase in the percent of arginine (4 versus 7%, p = 0.0006), aspartic acid (7 versus 11%, p = 0.0032), alanine (7 versus 13%, $p < 0.0001$), methionine (1 versus 3%, p = 0.0015), phenylalanine (1 versus 5%, $p < 0.0001$), and valine (2 versus 3%, p = 0.0354). Aged peritoneal PtC$^+$ B-1a cells display an increase in arginine (3 versus 5%, p = 0.0069), aspartic acid (7 versus 9%, p = 0.0140), and tryptophan (6 versus 10%, p = 0.0013), whereas these cells display a decrease in leucine (3 versus 2%, p = 0.0006). Aged splenic

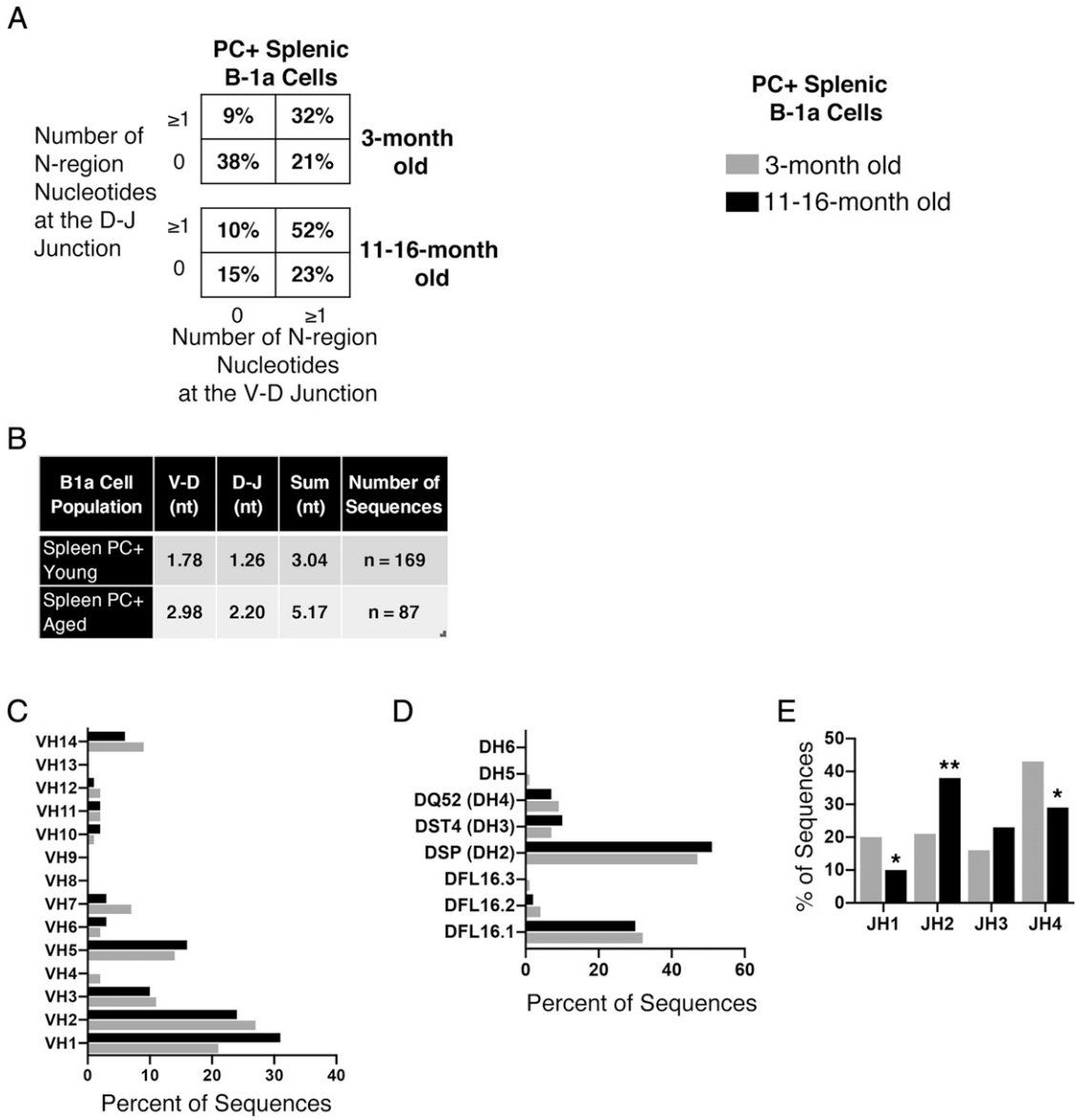

FIGURE 7. Splenic PC$^+$ B-1a cell IgM differs in germline status in middle-aged and young mice. Splenic PC$^+$ B-1a cells were single-cell sorted from 3- and 11- to 16-mo-old (as indicated) male BALB/c-ByJ mice. The V_H region was amplified and sequenced as detailed in *Materials and Methods*. (**A**) The percent of sequences with zero N-additions at both junctions is shown. (**B**) Average number of N-additions at the V-D, D-J, or sum of the two junctions. (**C**) The percent of V_H gene segment usage. (**D**) The percent of D_H gene segment usage. (**E**) The percent of J_H gene segment usage. Results are based on two independent experiments with sequences from 3-mo-old mice (n = 6) and 11- to 16-mo-old mice (n = 6). Statistics used: (A) 2 × 4 χ^2 test, (B) Mann–Whitney U test, and (C–E) 2 × 2 χ^2 test. *$p \leq 0.05$, **$p \leq 0.01$ (exact p values are defined in the text).

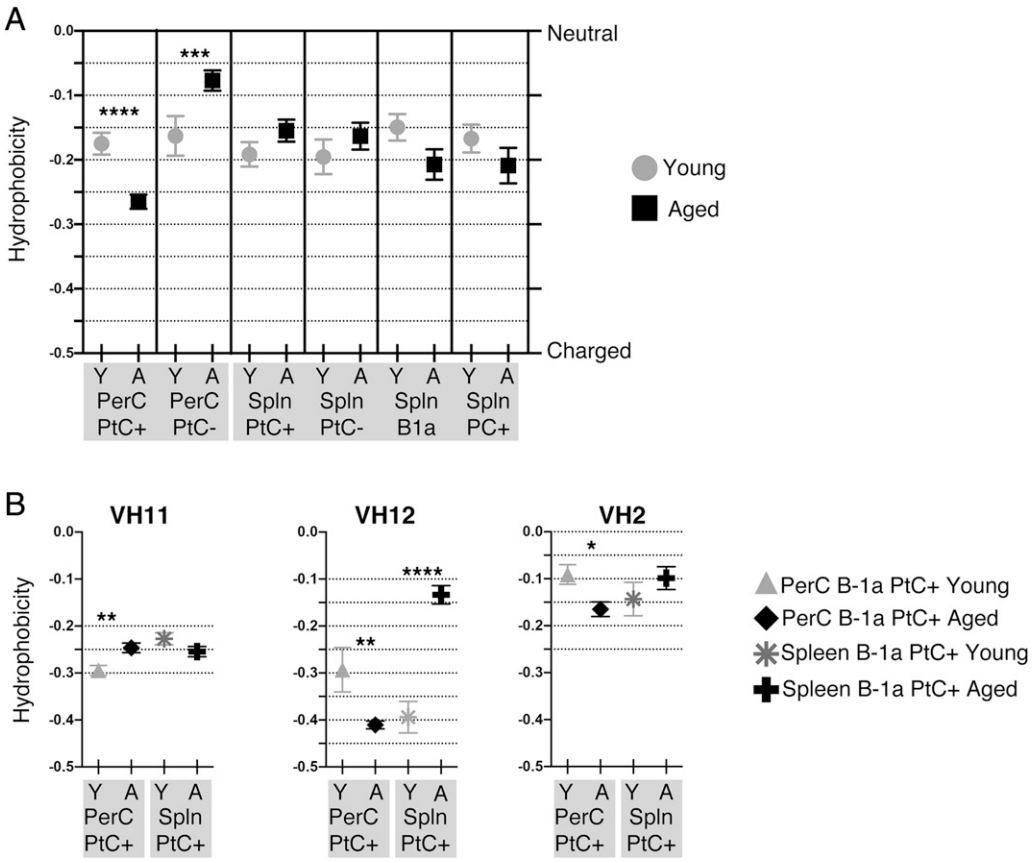

FIGURE 8. CDR-H3 hydrophobicity changes with age. Peritoneal or splenic B-1a cell populations were single-cell sorted from male BALB/c-ByJ mice as indicated. The V_H region was amplified and sequenced as detailed in *Materials and Methods*. (**A**) The average charge of the CDR-H3 loop region of IgM from indicated B-1a cell subset. (**B**) The average charge of the CDR-H3 loop region of IgM from peritoneal or splenic PtC^+ B-1a cells expressing V_H11, V_H12, or V_H2. These results are based on sequences obtained from experiments performed in Figs. 1, 3, 5, and 7 (see those figures for number of animals and independent experiment numbers). Statistics used: Mann–Whitney *U* test. $*p \leq 0.05$, $**p \leq 0.01$, $****p \leq 0.0001$ (exact *p* values are defined in the text).

PtC^+ B-1a cells display an increase in threonine (2 versus 4%, $p = 0.0104$). Aged splenic PtC^- B-1a cells show an increase in tryptophan (5 versus 8%, $p = 0.0058$). Aged splenic PC^+ B-1a cells display an increase in arginine (3 versus 5%, $p = 0.0422$). These results are shown in Fig. 9 and summarized in Supplemental Table I.

The changes observed in amino acid use within the CDR-H3 provide clues to how these populations are selected over time. An increase in arginine use is associated with an increase in autoreactive Abs (47, 53, 54). In this study, we demonstrate that peritoneal PtC^+ B-1a, peritoneal PtC B-1a, and splenic PC^+ B-1a cells have an increase in arginine use with age, suggesting these populations could contribute to an increase in autoantibodies with age. Next, it has been shown there are constraints upon the diversity of the CDR-H3 in terms of D_H reading frame (RF) use, the distribution of amino acids, and hydrophobicity. Such constraints include the following: 1) tyrosine and glycine within the CDR-H3 are primarily provided by D_H in RF1, 2) RF1 is normally favored, 3) DFL16.1 is the only D_H that encodes serine, 4) RF2 encodes hydrophobic amino acids, 5) DSP members either encode asparagine or aspartic acid in RF1, and 6) there is a preference for using less hydrophobic and less charged amino acids (55). Our results reflect such constraints. We observe a preference for less hydrophobic and less charged amino acids in all of the populations of B-1a cells examined in this study; however, peritoneal PtC^+ B-1a cells increase in overall charge with age (Fig. 8). We also see a predominance of DFL16.1 and DSP use in all populations of B-1a cells examined, and most show a preference for aspartic acid use (Fig. 9). Interestingly, when examining sequences using V_H11, asparagine is now preferentially used, whereas in sequences using V_H12 and V_H2, aspartic acid usage is preferred (Fig. 10). These findings reflect previous studies showing DSP gene segments using RF1 contain either asparagine or aspartic acid (55). Furthermore, the increased hydrophobicity seen in aged peritoneal PtC^- B-1a cells is accompanied by increases in hydrophobic amino acids (valine, alanine) and a decrease in tyrosine and glycine, which suggests an increase in RF2 use with age (Fig. 9). Interestingly, both splenic PtC^+ and PtC^- aged B-1a cells display a decrease in tyrosine, decrease in DFL16.1, and an increase in DQ52, suggesting a shift in RF use with age. Aged splenic PC^+ B-1a cells also display a decrease in tyrosine and a decrease in J_H4 use, again suggesting a shift in RF use with age. These changes in CDR-H3 amino acid content could have implications for B-1a cell function and ability to protect against infection in the aged mice.

As summarized in Supplemental Table I, the changes in hydrophobicity observed within these populations of B cells correlate with significant changes observed in either D_H usage, N-additions, and/or amino acid use within the CDR-H3. Therefore, the significant changes we observed in D usage, N-additions, amino acid use within the peritoneal and/or splenic B-1a cell populations examined in this study, resulted in a significant change in the CDR-H3 of these Abs.

Discussion

To gain a deeper understanding of how natural Abs change with age, we investigated whether age-related changes occur in Ag-specific,

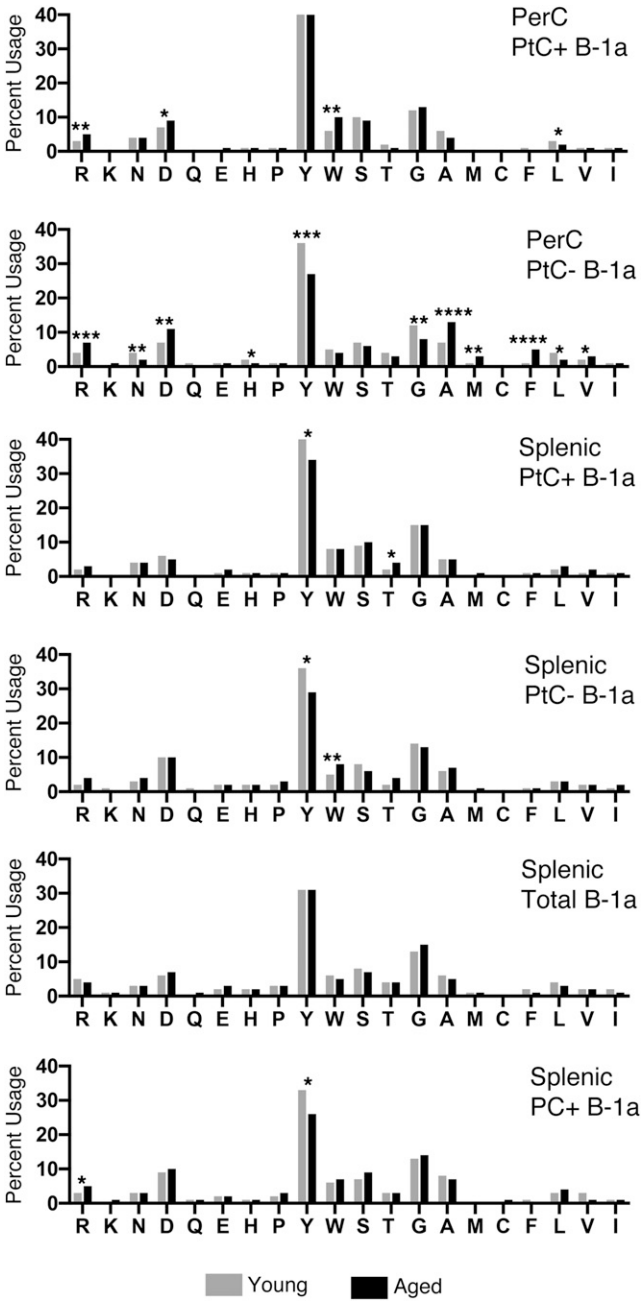

FIGURE 9. Amino acid distribution within the CDR-H3 changes with age. The percent of each amino acid used within the CDR-H3 was determined for each B-1a cell subset as indicated. These results are based on sequences obtained from experiments performed in Figs. 1, 3, 5, and 7 (see those figures for number of animals and independent experiment numbers). Statistics used: χ^2 test. *$p \leq 0.05$, **$p \leq 0.01$, ***$p \leq 0.001$, ****$p \leq 0.0001$ (exact p values are defined in the text).

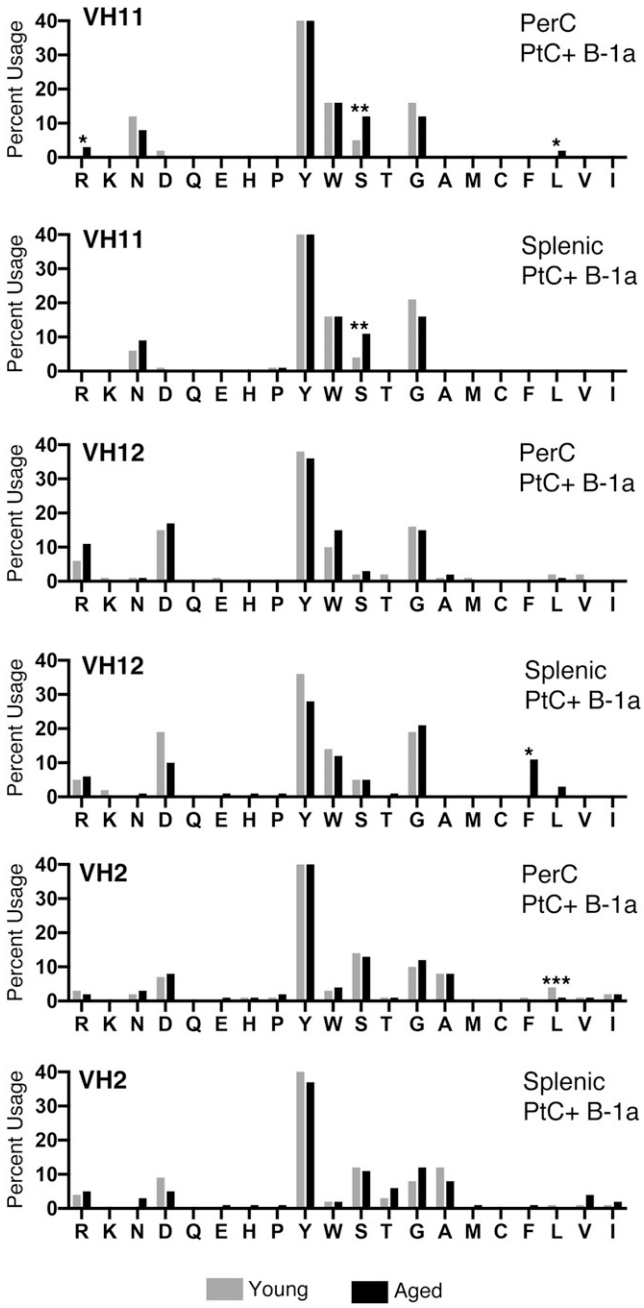

FIGURE 10. Amino acid distribution within the CDR-H3 of peritoneal and splenic PtC-binding B-1a cells using V_H11, V_H12, or V_H2. The percent of each amino acid used within the CDR-H3 was determined for each B-1a cell subset as indicated. These results are based on sequences obtained from experiments performed in Figs. 1, 3, 5, and 7 (see those figures for number of animals and independent experiment number). Statistics used: χ^2 test. *$p \leq 0.05$, **$p \leq 0.01$, ***$p \leq 0.001$ (exact p values are defined in the text).

B-1a cell–derived natural IgM. In this study, we found the germline-like nature (low–N-addition) of PtC-specific Ab from peritoneal cavity B-1a cells does not change with age (Fig. 1). In contrast, we found PtC-specific Ab from splenic B-1a cells moves away from germline with age (Fig. 3), which is similar to aged splenic (Fig. 7) and peritoneal (33) PC–specific B-1a cell IgM. Although peritoneal PtC^+ B-1a cells do not change in germline status with age, evidence of selection is still observed in a change of V_H use (Fig. 2), hydrophobicity (Fig. 8), and CDR-H3 amino acid content (Figs. 9, 10) with age. Our results demonstrate how selection differentially shapes the B-1a cell pool with increasing age, depending upon specificity and location.

The fact that selection shapes the B-1a cell pool over time is highlighted when considering peritoneal B-1a cells with PtC specificity. Results presented in Fig. 1 clearly demonstrate selective pressures acting upon peritoneal PtC^- B-1a cells with age do not have the same outcome on the peritoneal PtC^+ B-1a cells. In both young and aged mice, peritoneal PtC^+ B-1a cells retain a low level of N-addition (Fig. 1). These findings are in agreement with what is known about PtC-specific B cell development and

selection. It has been shown the PtC specificity encoded by V_H11 is at a developmental disadvantage during adult life (30). Lack of V_H11 use during bone marrow development occurs in part because of abundant N-additions during bone marrow lymphopoiesis, which disadvantages use of V_H11 (30). A lack of V_H11 use in PtC^+ bone marrow–derived B-1a cells has been demonstrated (32, 56). This finding is corroborated in our results, showing that the number of N-additions in IgM from peritoneal PtC^+ B-1a cells expressing V_H11 does not increase with age (Table III). The heavy chains V_H12 and V_H2 can also encode the PtC specificity and are more tolerant of N-additions (46), which we also observe (Table III). In the analysis of peritoneal PtC^+ B-1a cells presented in this study on average 87% of sequences use V_H11 (25%), V_H12 (7%), or V_H2 (55%) in 3-mo-old mice (Fig. 2A). In 15-to 18-mo-old mice, 86% of sequences use the same V_H segments but in different proportions: V_H11 (24%), V_H12 (31%), or V_H2 (31%) (Fig. 2A). Our findings demonstrating an increase in V_H12 with age (15- to 18-mo-old mice) in peritoneal PtC^+ B-1a cells are in agreement with previously published studies showing an age-dependent (1–7 mo) increase in V_H12 in peritoneal B-1 cells, which was shown to be Ag dependent (42). These results not only demonstrate oligoclonal expansion of V_H12 but also the contraction of V_H2. Such an expansion in V_H12 might be relevant to disease, as it was recently shown that aged $ApoE^{-/-}$ mice with established atherosclerosis have an expansion of a V_H12 specificity (AGDYDGYWYFDV) (57). We also observe this specificity within our aged peritoneal PtC^+ population but at a much lower frequency (Table I), which suggests Ag selection in the context of healthy aged versus $ApoE^{-/-}$ aged mice. Importantly, it has been previously shown that B cells are selected and accumulate in response to environmental Ags with age (58). Over time, during adult life, B cells are exposed to Ags, Abs, and other factors depending on where they reside, which could play a role in their maintenance and selection. This is exemplified by our examination of splenic PtC^+ B-1a cells.

PtC-binding B-1a cells are reported to be found at a low frequency in the spleen (1–2%) (43, 56). We also found a lower frequency of PtC-binding B-1a cells in the spleen compared with peritoneal cavity; however, we did observe more than 2% in spleens obtained from young (4.9% $\pm$ 0.84 SEM) and aged (10.3% $\pm$ 2.3 SEM) BALB/c-ByJ male mice (Fig. 3). A difference between peritoneal and splenic PtC^+ B-1a cells is also seen in terms of V_H use. On average 64% of sequences obtained from splenic PtC^+ B-1a cells use V_H11 (40%), V_H12 (5%), or V_H2 (19%) in 3-mo-old mice, and 59% of sequences use the same V_H segments but in different proportions: V_H11 (25%), V_H12 (9%), or V_H2 (25%) in 16- to 23-mo-old mice (Fig. 4). In contrast, 87% of young and 86% of aged peritoneal PtC^+ B-1a cells use V_H11, V_H12, or V_H2 (Fig. 2). Furthermore, hydrophobicity analyses of the CDR-H3 region reveals peritoneal (but not splenic) PtC^+ B-1 cells in the aged mice increase in charge, which is frequently seen in autoreactive Abs. There were also significant differences in overall amino acid content of peritoneal PtC^+ B-1a cells versus splenic PtC^+ B-1a cells when comparing young to young ($p = 0.0384$) and aged to aged mice ($p < 0.0001$). Together, these results showing differences in V_H use, hydrophobicity, and amino acid content between peritoneal and splenic PtC^+ B-1a cells demonstrate the consequence of differing selection pressures dependent upon location, specificity, and/or age (summarized in the visual abstract). Our findings suggest the differential selection of peritoneal and splenic B-1a cells is affected by Ag availability within the microenvironment in which they reside. The effects of Ag specificity in combination with the microenvironment has previously been shown in a PtC-specific–transgenic model system. This study demonstrated the responsiveness of PtC-specific B-1 cells was determined by the peritoneal or splenic microenvironment (59). Furthermore, splenic B-1 cells have been shown to associate with follicular dendritic cells (60). Such an association with dendritic cells could provide differential Ag exposure and subsequent selection of splenic B-1a cells, which peritoneal B-1a cells would not experience. Our results demonstrating the location and specificity of B-1a cells affect the germline-like structure and/or repertoire of B-1 cells with increasing age suggest differential Ag exposure plays a role in the selection of B-1a cells over time; however, further investigation is necessary to fully understand the mechanism of divergent selection in the peritoneal cavity and spleen. Essential to such future studies will be uncovering protective specificities (specific CDR-H3s and paired CDR-L3s) provided by PC, PtC, and/or Abs cross-reactive with both. A recent study in CB57BL/6 mice demonstrated the most frequently used CDR-H3 in peritoneal B-1a cells was a PtC specificity (MRYGNYWYFDV, using V_H11-D_H2-J_H1) that not only bound a classic PtC epitope but also bound PC and OxLDL (38), which are classically recognized by anti-PC Abs. We also find this specific CDR-H3 sequence most frequently used within the PtC^+ B-1a cells in both the spleen and peritoneal cavity of BALB/c-ByJ mice. These results demonstrate frequent use of this CDR-H3 in B-1a cells is conserved between the C57BL/6 and BALB/c-ByJ strains. It should also be noted that although the number of sequences within our analyses are somewhat limited because of performing single-cell sequencing, our results are consistent with studies using bulk sequencing approaches (38, 39).

Our results have implications for how therapeutic strategies and vaccines targeting B-1 cells should be approached for the aged (65 and over) population. We examined how the available PtC- and PC-specific natural IgM changes with age. Both natural IgM specificities have both been shown to be associated with protection against infections to which the elderly population is particularly susceptible, sepsis (14) and *S. pneumoniae* (13), respectively. Our results demonstrate the MRYGNYWYFDV CDR-H3 sequence is greatly diluted in the peritoneal compartment of aged mice (Tables I and II and Visual Abstract). The relative loss of this specific CDR-H3 might be important in terms of susceptibility to infection as well as vaccination strategies in the aged mice. Yet, other specificities such as V_H12 in the peritoneal PtC^+ B-1a cells were shown to increase in the aged population. These results demonstrate that there can be expansion and contraction within the B-1a cell pool over time. Therefore, B-1a cells are not a hermetically sealed population. Our results showing certain PtC specificities decrease while others increase with age suggests vaccination strategies for the aged population should be re-evaluated to favor expansion of B-1a cells producing protective Abs specificities; however, further work is needed to determine which specificities are most protective. In light of our results showing differential changes depending upon location, vaccination strategies should also take into account location of the target cells. In addition, these results suggest there might be fewer of such target cells within the aged population. Going forward, it will be essential to understand what role PtC-specific B-1a cells play in protection from infection as well as atherosclerosis, how these cells are maintained with age, and how they can be expanded to compensate for age-related loss and adverse selection.

Acknowledgments

We thank Selest Nashef for aiding in the design of the graphic for the visual abstract.

Disclosures

The authors have no financial conflicts of interest.

References

1. Ehrenstein, M. R., and C. A. Notley. 2010. The importance of natural IgM: scavenger, protector and regulator. *Nat. Rev. Immunol.* 10: 778–786.
2. Blandino, R., and N. Baumgarth. 2019. Secreted IgM: new tricks for an old molecule. *J. Leukoc. Biol.* 106: 1021–1034.
3. Holodick, N. E., N. Rodríguez-Zhurbenko, and A. M. Hernández. 2017. Defining natural antibodies. *Front. Immunol.* 8: 872.
4. Lalor, P. A., L. A. Herzenberg, S. Adams, and A. M. Stall. 1989. Feedback regulation of murine Ly-1 B cell development. *Eur. J. Immunol.* 19: 507–513.
5. Baumgarth, N. 2011. The double life of a B-1 cell: self-reactivity selects for protective effector functions. *Nat. Rev. Immunol.* 11: 34–46.
6. Boes, M., C. Esau, M. B. Fischer, T. Schmidt, M. Carroll, and J. Chen. 1998. Enhanced B-1 cell development, but impaired IgG antibody responses in mice deficient in secreted IgM. *J. Immunol.* 160: 4776–4787.
7. Nguyen, T. T., R. A. Elsner, and N. Baumgarth. 2015. Natural IgM prevents autoimmunity by enforcing B cell central tolerance induction. *J. Immunol.* 194: 1489–1502.
8. Tsiantoulas, D., M. Kiss, B. Bartolini-Gritti, A. Bergthaler, Z. Mallat, H. Jumaa, and C. J. Binder. 2017. Secreted IgM deficiency leads to increased BCR signaling that results in abnormal splenic B cell development. *Sci. Rep.* 7: 3540.
9. Ehrenstein, M. R., H. T. Cook, and M. S. Neuberger. 2000. Deficiency in serum immunoglobulin (Ig)M predisposes to development of IgG autoantibodies. *J. Exp. Med.* 191: 1253–1258.
10. Weksler, M. E., G. Pawelec, and C. Franceschi. 2009. Immune therapy for age-related diseases. *Trends Immunol.* 30: 344–350.
11. Binder, C. J., and G. J. Silverman. 2005. Natural antibodies and the autoimmunity of atherosclerosis. *Springer Semin. Immunopathol.* 26: 385–404.
12. Kearney, J. F., P. Patel, E. K. Stefanov, and R. G. King. 2015. Natural antibody repertoires: development and functional role in inhibiting allergic airway disease. *Annu. Rev. Immunol.* 33: 475–504.
13. Haas, K. M., J. C. Poe, D. A. Steeber, and T. F. Tedder. 2005. B-1a and B-1b cells exhibit distinct developmental requirements and have unique functional roles in innate and adaptive immunity to *S. pneumoniae*. *Immunity* 23: 7–18.
14. Boes, M., A. P. Prodeus, T. Schmidt, M. C. Carroll, and J. Chen. 1998. A critical role of natural immunoglobulin M in immediate defense against systemic bacterial infection. *J. Exp. Med.* 188: 2381–2386.
15. Centers for Disease Control and Prevention. 2017. Active bacterial core surveillance report, emerging infections program network, Streptococcus pneumoniae, 2017. Available at: https://www.cdc.gov/abcs/reports-findings/survreports/spneu17.html.
16. Centers for Disease Control and Prevention. 1997. Prevention of pneumococcal disease: recommendations of the advisory committee on immunization practices (ACIP). *MMWR Recomm. Rep.* 46: 1–24.
17. Jackson, L. A., K. M. Neuzil, O. Yu, P. Benson, W. E. Barlow, A. L. Adams, C. A. Hanson, L. D. Mahoney, D. K. Shay, and W. W. Thompson, Vaccine Safety Datalink. 2003. Effectiveness of pneumococcal polysaccharide vaccine in older adults. *N. Engl. J. Med.* 348: 1747–1755.
18. Ochoa-Gondar, O., A. Vila-Corcoles, X. Ansa, T. Rodriguez-Blanco, E. Salsench, C. de Diego, X. Raga, F. Gomez, E. Valdivieso, C. Fuentes, and L. Palacios, EVAN Study Group. 2008. Effectiveness of pneumococcal vaccination in older adults with chronic respiratory diseases: results of the EVAN-65 study. *Vaccine* 26: 1955–1962.
19. Johnstone, J., D. T. Eurich, J. K. Minhas, T. J. Marrie, and S. R. Majumdar. 2010. Impact of the pneumococcal vaccine on long-term morbidity and mortality of adults at high risk for pneumonia. *Clin. Infect. Dis.* 51: 15–22.
20. Kopf, M., B. Abel, A. Gallimore, M. Carroll, and M. F. Bachmann. 2002. Complement component C3 promotes T-cell priming and lung migration to control acute influenza virus infection. *Nat. Med.* 8: 373–378.
21. Baumgarth, N., O. C. Herman, G. C. Jager, L. E. Brown, L. A. Herzenberg, and J. Chen. 2000. B-1 and B-2 cell-derived immunoglobulin M antibodies are nonredundant components of the protective response to influenza virus infection. *J. Exp. Med.* 192: 271–280.
22. Nguyen, T. T. T., K. Kläsener, C. Zürn, P. A. Castillo, I. Brust-Mascher, D. M. Imai, C. L. Bevins, C. Reardon, M. Reth, and N. Baumgarth. 2017. The IgM receptor FcμR limits tonic BCR signaling by regulating expression of the IgM BCR. *Nat. Immunol.* 18: 321–333.
23. Masmoudi, H., T. Mota-Santos, F. Huetz, A. Coutinho, and P. A. Cazenave. 1990. All T15 Id-positive antibodies (but not the majority of VHT15+ antibodies) are produced by peritoneal CD5+ B lymphocytes. *Int. Immunol.* 2: 515–520.
24. Arnold, L. W., and G. Haughton. 1992. Autoantibodies to phosphatidylcholine. The murine antibromelain RBC response. *Ann. N. Y. Acad. Sci.* 651: 354–359.
25. Feeney, A. J. 1990. Lack of N regions in fetal and neonatal mouse immunoglobulin V-D-J junctional sequences. *J. Exp. Med.* 172: 1377–1390.
26. Kantor, A. B., C. E. Merrill, L. A. Herzenberg, and J. L. Hillson. 1997. An unbiased analysis of V(H)-D-J(H) sequences from B-1a, B-1b, and conventional B cells. *J. Immunol.* 158: 1175–1186.
27. Briles, D. E., C. Forman, S. Hudak, and J. L. Claflin. 1982. Anti-phosphorylcholine antibodies of the T15 idiotype are optimally protective against *Streptococcus pneumoniae*. *J. Exp. Med.* 156: 1177–1185.
28. Benedict, C. L., S. Gilfillan, T. H. Thai, and J. F. Kearney. 2000. Terminal deoxynucleotidyl transferase and repertoire development. *Immunol. Rev.* 175: 150–157.
29. Benedict, C. L., and J. F. Kearney. 1999. Increased junctional diversity in fetal B cells results in a loss of protective anti-phosphorylcholine antibodies in adult mice. *Immunity* 10: 607–617.
30. Hardy, R. R., C. J. Wei, and K. Hayakawa. 2004. Selection during development of VH11+ B cells: a model for natural autoantibody-producing CD5+ B cells. *Immunol. Rev.* 197: 60–74.
31. Gu, H., I. Förster, and K. Rajewsky. 1990. Sequence homologies, N sequence insertion and JH gene utilization in VHDJH joining: implications for the joining mechanism and the ontogenetic timing of Ly1 B cell and B-CLL progenitor generation. *EMBO J.* 9: 2133–2140.
32. Holodick, N. E., K. Repetny, X. Zhong, and T. L. Rothstein. 2009. Adult BM generates CD5+ B1 cells containing abundant N-region additions. *Eur. J. Immunol.* 39: 2383–2394.
33. Holodick, N. E., T. Vizconde, T. J. Hopkins, and T. L. Rothstein. 2016. Age-related decline in natural IgM function: diversification and selection of the B-1a cell pool with age. *J. Immunol.* 196: 4348–4357.
34. Alamyar, E., P. Duroux, M. P. Lefranc, and V. Giudicelli. 2012. IMGT(®) tools for the nucleotide analysis of immunoglobulin (IG) and T cell receptor (TR) V-(D)-J repertoires, polymorphisms, and IG mutations: IMGT/V-QUEST and IMGT/HighV-QUEST for NGS. *Methods Mol. Biol.* 882: 569–604.
35. Tiller, T., C. E. Busse, and H. Wardemann. 2009. Cloning and expression of murine Ig genes from single B cells. *J. Immunol. Methods* 350: 183–193.
36. Tumang, J. R., R. Francés, S. G. Yeo, and T. L. Rothstein. 2005. Spontaneously Ig-secreting B-1 cells violate the accepted paradigm for expression of differentiation-associated transcription factors. *J. Immunol.* 174: 3173–3177.
37. Mercolino, T. J., L. W. Arnold, and G. Haughton. 1986. Phosphatidyl choline is recognized by a series of Ly-1+ murine B cell lymphomas specific for erythrocyte membranes. *J. Exp. Med.* 163: 155–165.
38. Prohaska, T. A., X. Que, C. J. Diehl, S. Hendrikx, M. W. Chang, K. Jepsen, C. K. Glass, C. Benner, and J. L. Witztum. 2018. Massively parallel sequencing of peritoneal and splenic B cell repertoires highlights unique properties of B-1 cell antibodies. *J. Immunol.* 200: 1702–1717.
39. Yang, Y., C. Wang, Q. Yang, A. B. Kantor, H. Chu, E. E. Ghosn, G. Qin, S. K. Mazmanian, J. Han, and L. A. Herzenberg. 2015. Distinct mechanisms define murine B cell lineage immunoglobulin heavy chain (IgH) repertoires. *eLife* 4: e09083.
40. Malynn, B. A., G. D. Yancopoulos, J. E. Barth, C. A. Bona, and F. W. Alt. 1990. Biased expression of JH-proximal VH genes occurs in the newly generated repertoire of neonatal and adult mice. *J. Exp. Med.* 171: 843–859.
41. Khass, M., A. M. Vale, P. D. Burrows, and H. W. Schroeder, Jr. 2018. The sequences encoded by immunoglobulin diversity (D_H) gene segments play key roles in controlling B-cell development, antigen-binding site diversity, and antibody production. *Immunol. Rev.* 284: 106–119.
42. Herzenberg, L. A., N. Baumgarth, and J. A. Wilshire. 2000. B-1 cell origins and VH repertoire determination. *Curr. Top. Microbiol. Immunol.* 252: 3–13.
43. Baumgarth, N., E. E. Waffarn, and T. T. Nguyen. 2015. Natural and induced B-1 cell immunity to infections raises questions of nature versus nurture. *Ann. N. Y. Acad. Sci.* 1362: 188–199.
44. Holodick, N. E., T. Vizconde, and T. L. Rothstein. 2014. Splenic B-1a cells expressing CD138 spontaneously secrete large amounts of immunoglobulin in naïve mice. *Front. Immunol.* 5: 129.
45. Griffin, D. O., N. E. Holodick, and T. L. Rothstein. 2011. Human B1 cells in umbilical cord and adult peripheral blood express the novel phenotype CD20+ CD27+ CD43+ CD70-. [Published erratum appears in 2011 *J. Exp. Med.* 208: 871.]; [Published erratum appears in 2011 *J. Exp. Med.* 208: 409.]; [Published erratum appears in 2011 *J. Exp. Med.* 208: 67.] *J. Exp. Med.* 208: 67–80.
46. Seidl, K. J., J. A. Wilshire, J. D. MacKenzie, A. B. Kantor, L. A. Herzenberg, and L. A. Herzenberg. 1999. Predominant VH genes expressed in innate antibodies are associated with distinctive antigen-binding sites. *Proc. Natl. Acad. Sci. USA* 96: 2262–2267.
47. Krishnan, M. R., N. T. Jou, and T. N. Marion. 1996. Correlation between the amino acid position of arginine in VH-CDR3 and specificity for native DNA among autoimmune antibodies. *J. Immunol.* 157: 2430–2439.
48. Tonegawa, S. 1983. Somatic generation of antibody diversity. *Nature* 302: 575–581.
49. Zemlin, M., M. Klinger, J. Link, C. Zemlin, K. Bauer, J. A. Engler, H. W. Schroeder, Jr., and P. M. Kirkham. 2003. Expressed murine and human CDR-H3 intervals of equal length exhibit distinct repertoires that differ in their amino acid composition and predicted range of structures. *J. Mol. Biol.* 334: 733–749.
50. Ippolito, G. C., R. L. Schelonka, M. Zemlin, I. I. Ivanov, R. Kobayashi, C. Zemlin, G. L. Gartland, L. Nitschke, J. Pelkonen, K. Fujihashi, et al. 2006. Forced usage of positively charged amino acids in immunoglobulin CDR-H3 impairs B cell development and antibody production. *J. Exp. Med.* 203: 1567–1578.
51. Nguyen, H. H., M. Zemlin, I. I. Ivanov, J. Andrasi, C. Zemlin, H. L. Vu, R. Schelonka, H. W. Schroeder, Jr., and J. Mestecky. 2007. Heterosubtypic immunity to influenza A virus infection requires a properly diversified antibody repertoire. *J. Virol.* 81: 9331–9338.
52. Schelonka, R. L., M. Zemlin, R. Kobayashi, G. C. Ippolito, Y. Zhuang, G. L. Gartland, A. Szalai, K. Fujihashi, K. Rajewsky, and H. W. Schroeder, Jr. 2008. Preferential use of DH reading frame 2 alters B cell development and antigen-specific antibody production. *J. Immunol.* 181: 8409–8415.
53. Radic, M. Z., J. Mackle, J. Erikson, C. Mol, W. F. Anderson, and M. Weigert. 1993. Residues that mediate DNA binding of autoimmune antibodies. *J. Immunol.* 150: 4966–4977.
54. Silva-Sanchez, A., C. R. Liu, A. M. Vale, M. Khass, P. Kapoor, A. Elgavish, I. I. Ivanov, G. C. Ippolito, R. L. Schelonka, T. R. Schoeb, et al. 2015. Violation

of an evolutionarily conserved immunoglobulin diversity gene sequence preference promotes production of dsDNA-specific IgG antibodies. *PLoS One* 10: e0118171.
55. Schroeder, H. W., Jr., M. Zemlin, M. Khass, H. H. Nguyen, and R. L. Schelonka. 2010. Genetic control of DH reading frame and its effect on B-cell development and antigen-specifc antibody production. *Crit. Rev. Immunol.* 30: 327–344.
56. Düber, S., M. Hafner, M. Krey, S. Lienenklaus, B. Roy, E. Hobeika, M. Reth, T. Buch, A. Waisman, K. Kretschmer, and S. Weiss. 2009. Induction of B-cell development in adult mice reveals the ability of bone marrow to produce B-1a cells. *Blood* 114: 4960–4967.
57. Upadhye, A., P. Srikakulapu, A. Gonen, S. Hendrikx, H. M. Perry, A. Nguyen, C. McSkimming, M. A. Marshall, J. C. Garmey, A. M. Taylor, et al. 2019. Diversification and CXCR4-dependent establishment of the bone marrow B-1a cell pool governs atheroprotective IgM production linked to human coronary atherosclerosis. *Circ. Res.* 125: e55–e70.
58. Johnson, S. A., S. J. Rozzo, and J. C. Cambier. 2002. Aging-dependent exclusion of antigen-inexperienced cells from the peripheral B cell repertoire. *J. Immunol.* 168: 5014–5023.
59. Chumley, M. J., J. M. Dal Porto, and J. C. Cambier. 2002. The unique antigen receptor signaling phenotype of B-1 cells is influenced by locale but induced by antigen. *J. Immunol.* 169: 1735–1743.
60. Wen, L., S. A. Shinton, R. R. Hardy, and K. Hayakawa. 2005. Association of B-1 B cells with follicular dendritic cells in spleen. *J. Immunol.* 174: 6918–6926.